MLL5 maintains spindle bipolarity by preventing aberrant cytosolic aggregation of PLK1

Wei Zhao, Jie Liu, Xiaoming Zhang, and Lih-Wen Deng

Department of Biochemistry, Yong Loo Lin School of Medicine, National University of Singapore, Singapore 117597

Faithful chromosome segregation with bipolar spindle formation is critical for the maintenance of genomic stability. Perturbation of this process often leads to severe mitotic failure, contributing to tumorigenesis. MLL5 has been demonstrated to play vital roles in cell cycle progression and the maintenance of genomic stability. Here, we identify a novel interaction between MLL5 and PLK1 in the cytosol that is crucial for sustaining spindle bipolarity during mitosis. Knockdown of MLL5 caused aberrant PLK1 aggregation that led to acentrosomal microtubule-organizing center (aMTOC) formation and subsequent spindle multipolarity. Further molecular studies revealed that the polo-box domain (PBD) of PLK1 interacted with a binding motif on MLL5 (Thr887-Ser888-Thr889), and this interaction was essential for spindle bipolarity. Overexpression of wild-type MLL5 was able to rescue PLK1 mislocalization and aMTOC formation in MLL5-KD cells, whereas MLL5 mutants incapable of interacting with the PBD failed to do so. We thus propose that MLL5 preserves spindle bipolarity through maintaining cytosolic PLK1 in a nonaggregated form.

Introduction

The fidelity of mitosis, including the proper formation of bipolar spindles, is pivotal for genomic stability because it ensures faithful segregation of duplicated chromosomes to each daughter cell. Spindle multipolarity results in severe mitotic failures, such as DNA segregation errors and chromosome instability, leading to aneuploidy, a key feature of carcinogenesis (Fukasawa, 2007; Fang and Zhang, 2011; Vitre and Cleveland, 2012; Pihan, 2013). The centrosome is the main microtubule-organizing center (MTOC) and subsequently forms spindle poles in animal cells, where microtubules are nucleated and anchored. It consists of two cylindrical microtubule-based structures called centrioles surrounded by a protein matrix known as pericentriolar material (PCM; Bettencourt-Dias and Glover, 2007). The centriole duplicates once per cell cycle (during S phase), and additional PCM proteins are recruited to the centrosome for microtubule organization at the onset of mitosis (Dumont and Mitchison, 2009). Phosphorylation by protein kinases has long been considered a crucial mechanism of centrosome regulation (Fry et al., 2000). PLK1 functions as a master regulator of cell cycle progression and multiple cellular processes, including centrosome maturation and separation (Barr et al., 2004; Petronczki et al., 2008; Archambault and Glover, 2009). It promotes centrosome expansion by phosphorylating pericentrin and Nedd1 in human cells, Cnn in *Drosophila melanogaster*, and SPD-5 in *Caenorhabditis elegans* (Zhang et al., 2009a; Lee and Rhee, 2011; Conduit et al., 2014; Woodruff et al., 2015). The C-terminal polo-box domain (PBD) of PLK1 plays a vital role in targeting PLK1 kinase activity to specific subcellular localization (Elia et al., 2003a,b; Lowery et al., 2005). Moreover, PLK1 is involved in the formation of bipolar spindles, as indicated by the resulting monopolar spindle upon depletion or inhibition of PLK1 and the formation of multipolar spindles upon loss of PLK1 or its centrosomal substrates (Sumara et al., 2004; van Vugt et al., 2004; Oshimori et al., 2006; Lénárt et al., 2007; Ikeda et al., 2012).

The human gene for mixed lineage leukemia 5 (*MLL5*), a mammalian trithorax group gene, is located within a segment of chromosome 7q22, which is commonly deleted in acute myeloid leukemia and therapy-induced leukemia (Emerling et al., 2002). High MLL5 expression is associated with better clinical outcomes in acute myeloid leukemia patients (Damm et al., 2011). MLL5 contains a SET domain and a PHD zinc finger, which serves as a reader of H3K4me2 or H3K4me3 for MLL5 epigenetic regulation (Ali et al., 2013; Lemak et al., 2013). A recent study reported that MLL5 represses H3.3 expression and orchestrates global chromatin organization (Gallo et al., 2015). MLL5 has also been implicated in cell cycle control (Deng et al., 2004; Cheng et al., 2008, 2011; Sebastian et al., 2009; Zhou et al., 2013). Homozygous *Mll5*-null mice exhibit retarded growth, defects in hematopoietic function and homeostasis, and deregulated spermatogenesis (Heuser et al., 2009; Madan et al., 2009; Zhang et al., 2009b; Yap et al., 2011). Our previous

Correspondence to Lih-Wen Deng: bchdlw@nus.edu.sg

Abbreviations used in this paper: aMTOC, acentrosomal microtubule-organizing center; CD, central domain; co-IP, coimmunoprecipitation; CPC, chromosomal passenger complex; HSL, high-speed lysate; KD, knockdown; LSL, low-speed lysate; MLL5, mixed lineage leukemia 5; MTOC, microtubule-organizing center; NC, negative control; PBD, polo-box domain; PCM, pericentriolar material; PTM, posttranslational modification.

The Rockefeller University Press $30.00
J. Cell Biol. Vol. 212 No. 7 829–843
www.jcb.org/cgi/doi/10.1083/jcb.201501021

studies demonstrate that CDK1-catalyzed phosphorylation of MLL5 at the Thr-912 residue is required for mitotic entry and that regulation of the stability of the chromosomal passenger complex (CPC) by MLL5 contributes to genomic stability (Liu et al., 2010, 2012). We sought to determine the molecular mechanisms through which MLL5 maintains spindle bipolarity by studying its relationship with the key cell cycle regulator, PLK1.

Results

MLL5 is a centrosomal protein

We previously demonstrated that MLL5 maintains genomic stability through positively regulating the integrity of the CPC via a functional interaction with Borealin (Liu et al., 2012). Depletion of MLL5 results in multipolar-spindle formation with chromosome misalignment. Although ectopic overexpression of MLL5 could efficiently rescue these defects in MLL5 knockdown (KD) cells, restoration of CPC level alone could not correct spindle multipolarity (Liu et al., 2012). This would suggest a CPC-independent role of MLL5 in regulating spindle pole integrity. To test this possibility, we began with examining the centrosomal localization of endogenous MLL5 by costaining MLL5 with γ-tubulin in the human osteosarcoma U2OS cell line. At interphase, MLL5 localized to centrosomes as well as its known nuclear speckle localization (Deng et al., 2004), whereas during mitosis MLL5 delocalized from the nucleus to the cytoplasm but maintained its centrosomal localization (Fig. 1 A). The centrosomal localization of MLL5 during mitosis was confirmed with another two antibodies recognizing different regions of MLL5 (Fig. S1 A). Isolation of centrosomal fractions from U2OS cell lysates using sucrose density-gradient ultracentrifugation confirmed that endogenous MLL5 and γ-tubulin were found in the same fractions (Fig. 1 B). To explore whether endogenous MLL5 could interact with known centrosomal proteins, we performed coimmunoprecipitation (co-IP) studies in U2OS cell lysates with either anti-MLL5 or anti–rabbit IgG antibody, and the eluates were subjected to Western blotting. As shown in Fig. 1 C, an interaction between endogenous MLL5 and γ-tubulin was detected. Similarly, binding of γ-tubulin to FLAG-MLL5 could be detected in 293T cells expressing FLAG-MLL5 (Fig. 1 D). The construction and overexpression of three deletion mutants of MLL5 followed by co-IP studies revealed that the central domain (CD) of MLL5, rather than the PHD/SET domain or the C-terminal domain, was responsible for the γ-tubulin binding (Fig. 1, E and F). Notably, a slower-migrating form of FLAG-MLL5-CD (Fig. 1 F, arrowhead) could also be pulled down by the anti–γ-tubulin antibody. Because phosphatase treatment demonstrated that the slower gel mobility of MLL5 at G_2/M phase was caused by phosphorylation (Liu et al., 2010), posttranslational modification (PTM), particularly phosphorylation, on MLL5-CD is likely to contribute to MLL5 centrosomal function.

Down-regulation of MLL5 induces aMTOC formation, resulting in spindle multipolarity

Next, we examined the effect of down-regulation of MLL5 on mitotic spindle formation. U2OS cells were transfected with either negative control (NC)– or MLL5-specific siRNA for 24 h (Cheng et al., 2008), followed by synchronization to prometaphase with nocodazole treatment. Cells were released into nocodazole-free medium and further arrested at metaphase with the proteasome inhibitor MG132. Endogenous MLL5 was efficiently down-regulated after siRNA transfection (Fig. S1 B). Immunostaining with anti-pericentrin and anti–α-tubulin antibodies revealed that the knockdown of MLL5 increased the proportion of cells with more than two centrosome markers and multipolar spindles up to sevenfold at metaphase (NC-siRNA: 9.0%; MLL5-siRNA: 63.3%, P = 0.002; Fig. 2, A and D; and Videos 1 [NC-siRNA] and 2 [MLL5-siRNA]). This multipolar-spindle phenotype was also observed in normal diploid fibroblast WI-38 cells and the cervical cancer HeLa cell line (Fig. S1, C and D). It is worth mentioning that such multiple centrosome markers were observed predominantly at metaphase but not at prometaphase (NC: 4.0%; MLL5-siRNA: 3.3%; Fig. 2, B and D), implying that MLL5-KD cells underwent normal centrosome duplication and entered mitosis with two centrosomes containing a pair of centrioles each (Fig. 2 B, insets). Moreover, microtubule depolymerization at metaphase did not cause the multiple centrosome markers to coalesce into two foci, and the proportion of cells with more than two centrosome markers remained significantly higher in the MLL5-KD group compared with the control group (NC-siRNA: 3.7%; MLL5-siRNA: 52.7%, P = 0.002; Fig. 2, C and D). This suggests that the centrosome abnormalities occurring in MLL5-KD cells were unlikely to be caused by centrosome fragmentation and were microtubule independent. To delineate how multipolar spindles are formed in MLL5-KD cells, we monitored U2OS cells stably expressing GFP-tagged α-tubulin by time-lapse microscopy. In addition to the initial two MTOCs in the control cells, we observed that additional MTOCs appeared in MLL5-KD cells during microtubule nucleation, leading to spindle multipolarity (Fig. 2 E and Videos 3 [NC-siRNA] and 4 [MLL5-siRNA]). To verify whether these additional MTOCs are indeed functional, microtubule regrowth assays were performed. Cells at metaphase were incubated with ice-cold medium to achieve microtubule depolymerization. After release from the cold treatment, the majority of MLL5-KD cells still displayed multipolar spindles with multiple centrosome markers, implying that those additional MTOCs were able to organize spindles (Fig. S1, E and F). Next, we imaged PCM proteins and the centrioles to examine whether the formation of additional MTOCs was centriole dependent. In MLL5-KD cells, both pericentrin and γ-tubulin consistently colocalized to form supernumerary foci (Fig. 2 F). Yet, only two of these foci showed the presence of a pair of centrin-2 spots (Fig. 2 G). Collectively, those additional MTOCs responsible for the formation of multipolar spindles in MLL5-KD cells did not originate from the centrioles and were therefore acentrosomal MTOCs (aMTOCs).

Knockdown of MLL5 leads to aberrant cytosolic aggregation of PLK1

PLK1 has been demonstrated to control microtubule-based microtubule nucleation (Johmura et al., 2011). During mitosis, PLK1 is enriched at the centrosome and the subsequent kinetochore (Petronczki et al., 2008). Immunofluorescence showed that MLL5 colocalized with PLK1 at the centrosome during metaphase, and isolation of centrosomal fractions demonstrated that PLK1 and MLL5 coexisted in the same fractions as γ-tubulin (Fig. S2, A and B). Next, we asked whether MLL5 has any effects on PLK1 expression or its subcellular localization. There was no significant difference in PLK1 total protein levels between NC- and MLL5-siRNA–transfected mitotic cells (Fig. S2 C). Interestingly, down-regulation of MLL5 greatly increased

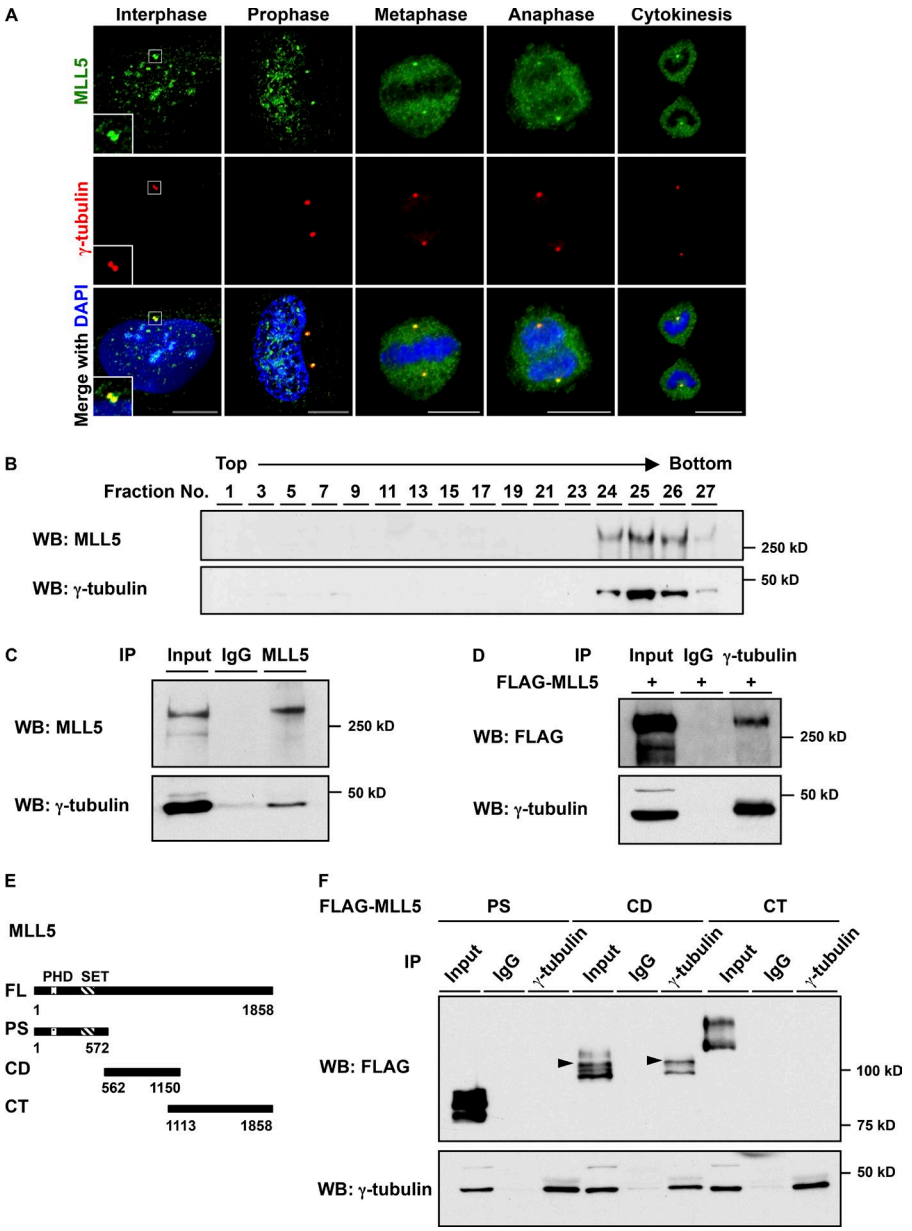

Figure 1. **MLL5 is a centrosomal protein.** (A) MLL5 centrosomal localization. U2OS cells were immunostained for MLL5 (green) and γ-tubulin (red). DNA was counterstained with DAPI (blue). Bars, 10 µm. Insets show high-magnification (2.5×) images of the centrosome at interphase. (B) Sucrose gradient centrifugation isolating the centrosome components. Fractions with concentrations ranging from 40% to 60% were collected and detected by Western blotting (WB) with anti-MLL5 and anti–γ-tubulin antibodies. (C) Interaction between endogenous MLL5 and γ-tubulin. After synchronization to prometaphase by nocodazole treatment, U2OS cell lysates were immunoprecipitated with anti-MLL5 antibody or mouse IgG and detected by Western blotting with anti-MLL5 and anti–γ-tubulin antibodies. (D) Interaction between FLAG-MLL5 and γ-tubulin. 293T cells expressing FLAG-MLL5 were synchronized to prometaphase by nocodazole treatment before immunoprecipitation and Western blotting. (E) Schematic representation of truncated MLL5 mutants. PS, PHD/SET domain; CT, C-terminal domain. (F) The central domain of MLL5 binding to γ-tubulin. 293T cells expressing FLAG-MLL5-PS, FLAG-MLL5-CD, or FLAG-MLL5-CT were synchronized to prometaphase before immunoprecipitation and Western blotting. Arrowhead indicates a slow-migrating form of FLAG-MLL5-CD. Results in B–D and F are representative of at least three experimental repeats.

the proportion of cells with PLK1 aggregates that did not colocalize with either the centrosome (indicated by pericentrin) or the kinetochore (indicated by CREST staining; Fig. 3, A–C; $P = 0.005$). After cells were released from prometaphase, multiple centrosome markers were observed in MLL5-KD cells at metaphase, which is consistent with previous results. Moreover, PLK1 localized to each of the centrosome markers indicated by pericentrin (Fig. 3 D, arrow; and Videos 5 [NC-siRNA] and 6 and 7 [MLL5-siRNA]), suggesting the involvement of PLK1 aggregates in the establishment of aMTOCs that formed extra spindle poles. Nevertheless, not all PLK1 aggregates resulted in the formation of new spindle poles as MLL5-KD cells with multiple centrosome markers still contained PLK1 aggregates that neither localized to pericentrin nor overlapped with DAPI staining (Fig. 3 D, arrowhead). Further costaining of pericentrin and PLK1 indicated a significantly reduced intensity of centrosomal PLK1 fluorescence in MLL5-KD cells at prometaphase (Fig. 3, E and F; $P < 0.001$), indicating partial dissociation of PLK1 from the centrosome. In line with this, costaining of centrin-2 and PLK1 at metaphase showed that the fluorescence intensity of centriole-localized PLK1 was also drastically reduced in MLL5-KD cells (Fig. S2 D). Collectively, knockdown of MLL5 caused aberrant cytosolic aggregation of PLK1 and its partial dissociation from the centrosome during mitosis.

Cytosolic interaction between MLL5 and PLK1 is required for spindle bipolarity

One possible explanation for PLK1 mislocalization in the MLL5-KD cells could be that centrosomal MLL5 is required for PLK1 recruitment to the centrosome. However, the observation that PLK1 still partially localized to the centrosome in the MLL5-KD cells argues against this hypothesis (Fig. 3, E and F). Because MLL5 delocalizes from the nucleus to the cytoplasm but maintains its centrosomal localization during mitosis, it is plausible that cytosolic MLL5 plays a role in preventing PLK1 from mislocalization. To test this hypothesis, we first depleted centrosomal MLL5 by eliminating the centrosome via PLK4 KD (Habedanck et al., 2005). The majority of PLK4-siRNA–

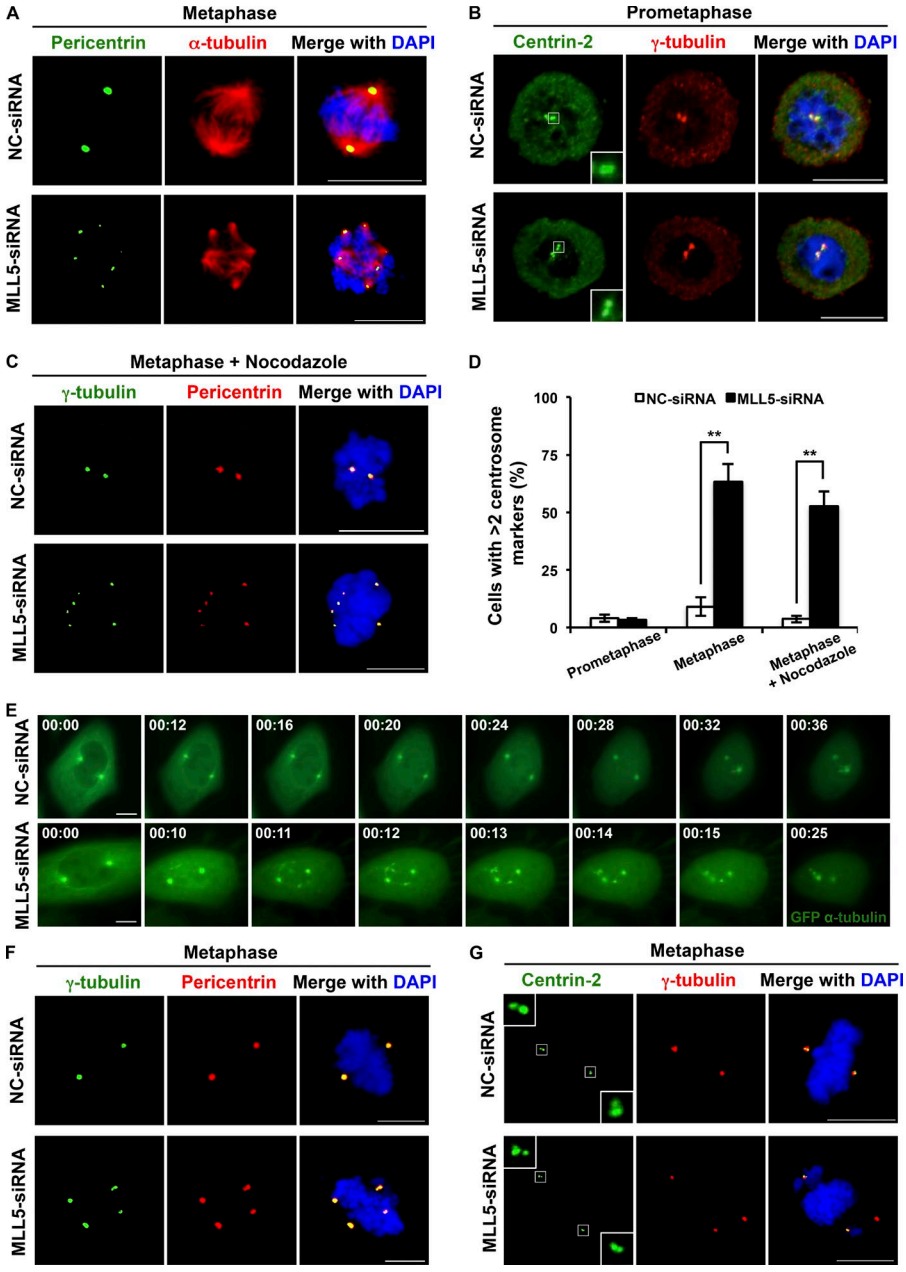

Figure 2. **Down-regulation of MLL5 causes multipolar spindle formation.** (A) Spindle multipolarity in MLL5-KD cells at metaphase. U2OS cells transfected with NC- or MLL5-siRNA were synchronized to metaphase and immunostained for pericentrin (green) and α-tubulin (red). (B) Two centrosomes in control and MLL5-KD cells at prometaphase. U2OS cells transfected with NC- or MLL5-siRNA were synchronized to prometaphase and immunostained for centrin-2 (green) and γ-tubulin (red). Insets show high-magnification (2.5×) images of a pair of centrioles. (C) Multiple centrosomes in MLL5-KD cells at metaphase after microtubule depolymerization. U2OS cells transfected with NC- or MLL5-siRNA were synchronized to metaphase, treated with nocodazole for 1 h to depolymerize microtubules, and immunostained for γ-tubulin (green) and pericentrin (red). (D) Quantitation of the data presented in A–C. The experiments were repeated three times (n = 100 cells per sample). Error bars represent SEM. **, $P < 0.01$. (E) Extra MTOC formation in MLL5-KD cells expressing GFP–α-tubulin. U2OS cells stably expressing GFP–α-tubulin were transfected with NC- or MLL5-siRNA for 48 h, and images were taken from prophase to metaphase. Frames taken at the indicated time points (h:min) are shown. (F and G) Multiple PCM foci and two pairs of centrioles are present in MLL5-KD cells. U2OS cells transfected with NC- or MLL5-siRNA were synchronized to metaphase and immunostained for γ-tubulin (green) and pericentrin (red) or for centrin-2 (green) and γ-tubulin (red). Inset in G shows high-magnification (2.5×) image of a pair of centrioles. Bars, 10 µm. DNA in A–C, F, and G was counterstained with DAPI (blue).

transfected U2OS cells were arrested at interphase, whereas among those successfully synchronized to metaphase, 49% displayed one centrosome and 22% had no centrosomes (Fig. S2 E). In the PLK4-depleted cells with acentrosomal spindles, centrosome-localized MLL5 was successfully eliminated (Fig. S2 F). Interestingly, loss of centrosomal MLL5 in PLK4-KD cells did not result in a drastic increase in the cells with cytosolic PLK1 aggregates (Fig. 4, A [left] and B; $P > 0.05$, NC-siRNA vs. PLK4-siRNA). Moreover, the percentage of cells with multipolar spindles remained low in the centrosome-depleted cells (Fig. 4, C [left] and D; $P > 0.05$, NC-siRNA vs. PLK4-siRNA). These results indicate that centrosomal MLL5 was not essential for keeping PLK1 in a nonaggregated form and not required for maintaining spindle bipolarity. Next, we depleted cytosolic MLL5 in these NC- or PLK4-siRNA–transfected U2OS cells and examined the effects on PLK1 aggregation and spindle bipolarity. To increase MLL5-KD efficiency in the centrosome-depleted cells, NC- or PLK4-siRNA–transfected cells were transduced with NC- or MLL5-shRNA by lentivirus infection for 24 h before synchronization to metaphase by nocodazole-MG132 treatment. Both PLK4 and MLL5 were greatly down-regulated after siRNA/shRNA treatment (Fig. S2 G). Strikingly, down-regulation of cytosolic MLL5 led to significantly elevated levels of cells displaying cytosolic PLK1 aggregates in spite of the number of the centrosome (Fig. 4, A [arrowhead] and B; $P < 0.001$, NC-shRNA vs. MLL5-shRNA). Furthermore, the percentage of cells with multipolar spindles became dramatically higher upon knockdown of cytosolic MLL5 (Fig. 4, C and D; $P < 0.001$, NC-shRNA vs. MLL5-shRNA). Collectively, cytosolic MLL5 rather than centrosomal MLL5 is required for the prevention of aberrant PLK1 aggregation and is crucial for the maintenance of bipolar spindle formation during mitosis.

To verify whether MLL5 interacts with PLK1 in the cytosol, U2OS cells or 293T cells expressing FLAG-MLL5 and HA-PLK1 were synchronized to mitosis. Cell lysates were first

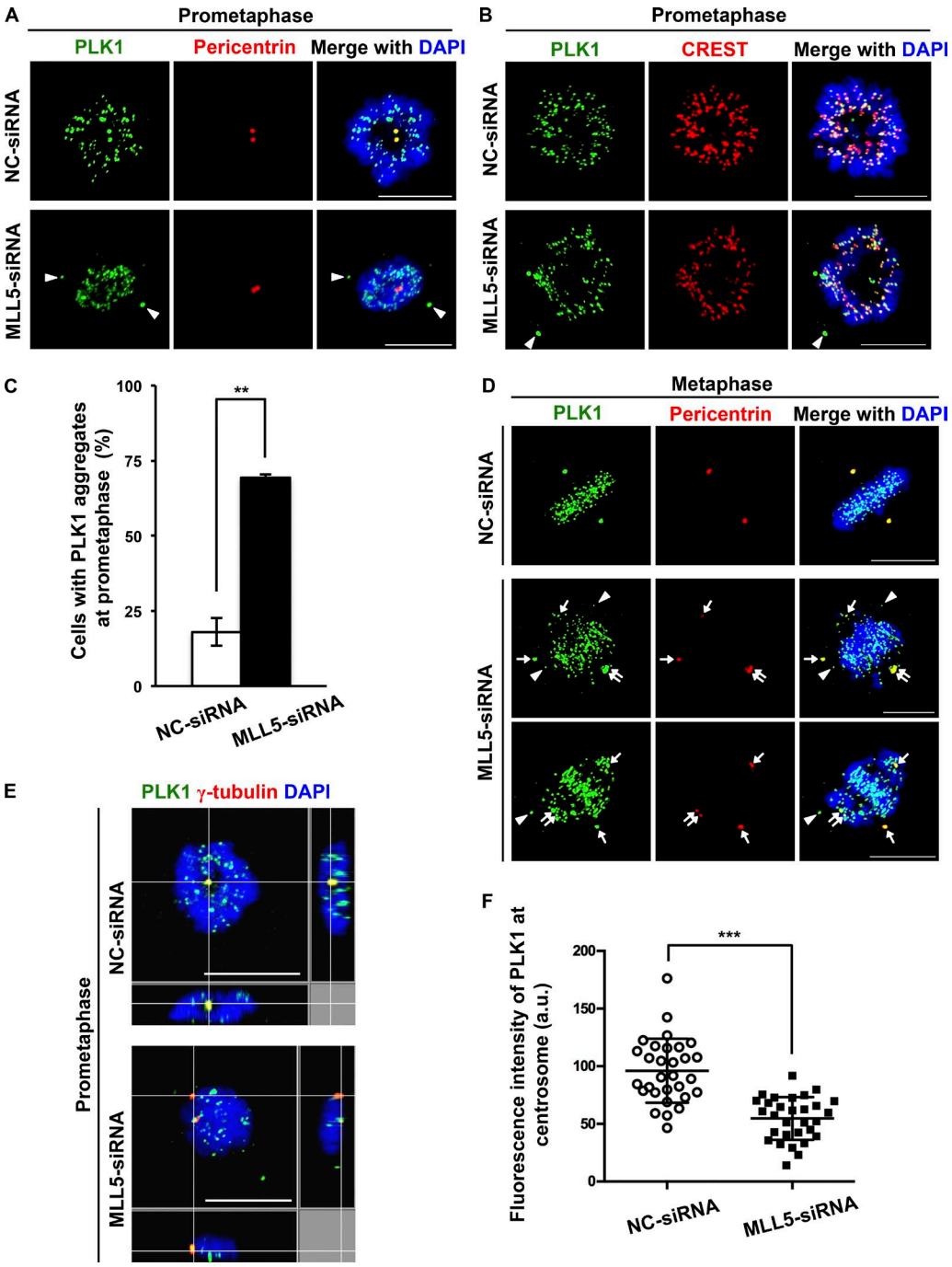

Figure 3. **Knockdown of MLL5 leads to aberrant cytosolic aggregation of PLK1.** (A and B) PLK1 aggregation in MLL5-KD cells at prometaphase. U2OS cells transfected with NC- or MLL5-siRNA were synchronized to prometaphase and immunostained for PLK1 (green) and pericentrin (red) or PLK1 (green) and CREST (red). Arrowhead indicates PLK1 aggregate. (C) Quantitation of cells with PLK1 aggregates in A. Experiments were repeated three times (n = 100 cells per sample). Error bars represent SEM. **, P = 0.005. (D) Colocalization of PLK1 and pericentrin. Cells transfected with NC- or MLL5-siRNA were synchronized to metaphase and immunostained for PLK1 (green) and pericentrin (red). Arrow indicates colocalization of PLK1 and pericentrin. Arrowhead indicates PLK1 aggregate. (E) Reduced intensity of centrosomal PLK1 in MLL5-KD cells at prometaphase. U2OS cells transfected with NC- or MLL5-siRNA were synchronized to prometaphase and immunostained for PLK1 (green) and γ-tubulin (red). (F) Quantitation of centrosomal PLK1 signal at prometaphase (a.u., arbitrary unit). Thirty cells were captured per sample manually, and mean pixel intensity of PLK1 was computed. ***, P < 0.001. Bars, 10 µm. DNA in A, B, D, and E was counterstained with DAPI (blue).

centrifuged at 12,000 *g*, and the collected supernatants were further subjected to ultracentrifugation (95,000 rpm; TLA100.3 rotor) to remove the remaining centrosome fragments. Co-IP was performed in both low-speed lysate (LSL) containing centrosomes and high-speed lysate (HSL) lacking centrosomes (Gopalakrishnan et al., 2011; Wueseke et al., 2014). As shown in Fig. 4 E, endogenous PLK1 was coimmunoprecipitated with endogenous MLL5 not only in LSL but also in HSL, confirming the cytosolic interaction between MLL5 and PLK1. Likewise, HA-PLK1 could be pulled down by FLAG-MLL5 in both LSL

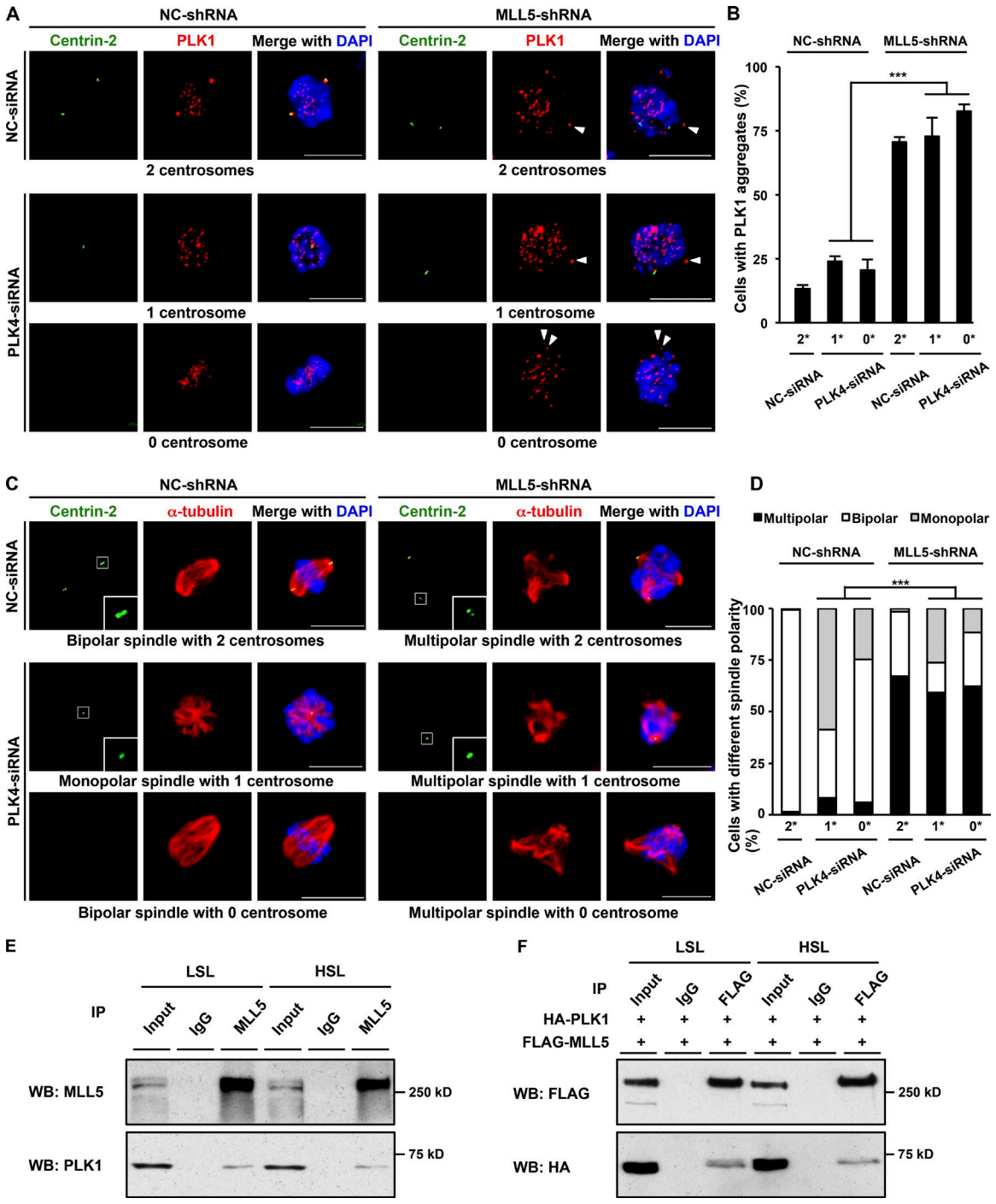

Figure 4. **Cytosolic interaction between MLL5 and PLK1 is required for spindle bipolarity.** (A) An increase in PLK1 aggregates after down-regulation of cytosolic MLL5. U2OS cells were transfected with NC- or PLK4-siRNA for 24 h and further transduced with NC- or MLL5-shRNA through lentiviral infection for another 24 h. Cells were then synchronized to metaphase by nocodazole-MG132 treatment and immunostained for PLK1 (red) and centrin-2 (green). Arrowhead indicates PLK1 aggregate. (B) Quantitation of cells with PLK1 aggregates in A. The experiments were repeated three times (n = 50 cells per sample). Error bars represent SEM. 2*, 2 centrosomes; 1*, 1 centrosome; 0*, 0 centrosome. ***, $P < 0.001$. (C) An increase in multipolar spindles after down-regulation of cytosolic MLL5. U2OS cells were introduced with NC- or PLK4-siRNA for 24 h and NC- or MLL5-shRNA for another 24 h. Cells were then synchronized to metaphase and immunostained for α-tubulin (red) and centrin-2 (green). Insets show high-magnification (2.5×) images of centrioles. (D) Quantitation of cells with monopolar, bipolar, and multipolar spindles in C. The experiments were repeated three times (n = 50 cells per sample). 2*, 2 centrosomes; 1*, 1 centrosome; 0*, 0 centrosome. ***, $P < 0.001$. (E) Cytosolic interaction between MLL5 and PLK1 during mitosis. Mitotic U2OS cell lysates were ultracentrifuged at 95,000 rpm with a TLA100.3 rotor after low-speed centrifugation (12,000 *g*). Supernatants before (LSL) and after (HSL) ultracentrifugation were then immunoprecipitated with anti-MLL5 antibody or rabbit IgG and detected by Western blotting with anti-MLL5 and anti-PLK1 antibodies. (F) Cytosolic interaction between FLAG-MLL5 and HA-PLK1 during mitosis. HSL and LSL of 293T cells coexpressing FLAG-MLL5 and HA-PLK1 were immunoprecipitated with anti-FLAG antibody or mouse IgG and detected by Western blotting (WB) with anti-FLAG and anti-HA antibodies. Bars, 10 µm. DNA in A and C was counterstained with DAPI (blue). Results in E and F are representative of at least two experimental repeats.

and HSL (Fig. 4 F). Collectively, the cytosolic interaction between MLL5 and PLK1 at mitosis prevented cytosolic aggregation of PLK1 and spindle multipolarity.

The PLK1 PBD interacts with the Thr887-Ser888-Thr889 motif on MLL5

To assess which part of MLL5 binds to PLK1 during mitosis, truncated FLAG-MLL5 mutants and HA-tagged PLK1 were coexpressed in 293T cells before synchronization to prometaphase. Co-IP showed that, in agreement with the interaction between MLL5 and γ-tubulin, HA-PLK1 bound only to the central domain of MLL5 including the slower-migrating form, which is MLL5-CD with relatively more PTMs (Fig. 5 A). In line with previous results, removal of centrosome fragments by ultracentrifugation did not abrogate such binding, indicating a cytosolic interaction between MLL5-CD and PLK1 during mitosis (Fig. S3 A). The PBD of PLK1 is known to direct PLK1 to specific subcellular localization through binding to other proteins (Petronczki et al., 2008). As shown in Fig. 5 B, PBD-mutated PLK1 (H538A-K540M; Elia et al., 2003b) failed to interact with the slower-migrating form of MLL5-CD, whereas wild-type PLK1 or kinase-dead PLK1 (D194A) bound to both forms. Thus, we propose that MLL5-CD comprises a binding site with PTM for MLL5 interaction with the PLK1 PBD. To map the region of MLL5-CD responsible for the PBD binding, two smaller FLAG-MLL5 fragments (CD6 and CD9; Liu et al., 2010) were coexpressed with either wild-type HA-PLK1 or PBD-mutated HA-PLK1. The slowest-migrating form of MLL5-CD9 (aa 818–984; Fig. S3 B, arrow) maintained its ability to bind wild-type PLK1 but not PBD-mutated PLK1 (Fig. S3 B), suggesting the location of the PBD-binding site within MLL5-CD9. CDK1, verified as a prodirected kinase responsible for the phosphorylation of a variety of PLK1 targets (Elia et al., 2003a; Preisinger et al., 2005; Neef et al., 2007; Ikeda et al., 2012), phosphorylates MLL5 at Thr-912 at the onset of mitosis (Liu et al., 2010). However, T912A mutation did not affect MLL5 interaction with PLK1, indicating that Thr-912 is not the PBD-binding site on MLL5 (Fig. S3 C). According to the consensus-binding sequence for the PLK1 PBD interaction, five putative binding sites on MLL5-CD9 were identified (Elia et al., 2003a; Lowery et al., 2007). We initially screened five double or triple alanine mutants, of which only the CD4-TST887AAA triple alanine mutant displayed marked reduction in its interaction with the PLK1 PBD (Fig. 5 C). Further dissection into three single-site mutants revealed that substituting any of the Thr-887, Ser-888, or Thr889 residues with alanine reduced the PLK1 interaction with MLL5, and the S888A mutant showed the most significant loss of PBD binding, comparable to that of TST887AAA (Fig. 5 D), indicating that Ser-888 is the key binding residue for PLK1. However, phosphorylation of this motif by a priming kinase appeared not to be necessary for PBD binding, as MLL5 mutants mimicking phosphorylation on Thr-887, Ser-888, or Thr-889 also displayed significant loss of binding to the PBD of PLK1 (Fig. S3 D).

PLK1 phosphorylates MLL5 on Ser-861

Because the PBD of PLK1 binds to the Thr887-Ser888-Thr889 motif on MLL5, we examined whether PLK1 also phosphorylates MLL5 by gel mobility shift assay. 293T cells expressing FLAG-MLL5-CD were synchronized to G_2 phase using the CDK1 inhibitor RO3306 or to prometaphase with nocodazole. The cells arrested at prometaphase were further incubated with or without the PLK1 inhibitor BI2536 and subjected to Western blotting. Consistently, the slower-migrating form of MLL5-CD (Fig. 6 A, arrow) appeared after the cells entered mitosis, which migrated faster in the presence of BI2536 (Fig. 6 A, top), demonstrating that the central domain of MLL5 was phosphorylated by PLK1 at the onset of mitosis. Moreover, FLAG-MLL5-CD4 showed multiple forms with different mobility, among which the slowest-migrating form moved faster under BI2536 treatment (Fig. 6 A, bottom). This suggests that the phosphorylation of MLL5 by PLK1 occurred within the CD4 domain of MLL5.

Next, an in vitro PLK1 kinase assay was performed using GST and GST-fused recombinant MLL5-CD4 purified from *Escherichia coli*. As revealed in Fig. 6 B, PLK1 phosphorylated MLL5-CD4 or casein but not GST, and inhibition of PLK1 with BI2536 abrogated the phosphorylation. To identify the specific PLK1 phospho-site on MLL5, mass spectrometry analyzing the products of in vitro kinase assay was performed. The results showed that PLK1 phosphorylated MLL5 at Ser-861 (Fig. S4 A). To confirm this, a S861A mutant was subjected to gel mobility shift assay. Western blotting clearly demonstrated that the slowest-migrating form of MLL5-CD4-S861A moved equally fast with or without BI2536 at mitosis (Fig. 6 C, top), indicating that the mutation of Ser-861 to alanine had abrogated PLK1 phosphorylation before BI2536 treatment. Nevertheless, mutation of the PBD binding motif Thr887-Ser888-Thr889 to alanine did not prevent PLK1 phosphorylation of MLL5 (Fig. 6 C, bottom), indicating that the PBD binding to Thr887-Ser888-Thr889 was not essential for PLK1 phosphorylation of MLL5 on Ser-861.

Exogenous overexpression of MLL5 rescues cells from PLK1 mislocalization and aMTOC formation in MLL5-KD cells

To assess whether PLK1 phosphorylation of MLL5 or PBD binding to MLL5 is essential for PLK1 centrosomal localization and spindle bipolarity, we ectopically introduced FLAG-MLL5 or mutant MLL5 constructs to MLL5-KD cells. 293T cells were treated with MLL5-siRNA for 16 h to knock down endogenous MLL5, followed by transfection with FLAG-MLL5 or its mutant for a further 8 h. Cells were subsequently synchronized to prometaphase by monastrol for PLK1 and MLL5 staining or to metaphase by nocodazole-MG132 treatment for pericentrin and MLL5 staining. Cells arrested at prometaphase with monastrol showed characteristic monopolar spindles with the centrosome located at the center of the cell, as indicated by the presence of centrosomal FLAG-MLL5 (Fig. 7 A). PLK1 foci in the periphery of the cell, exclusive of DNA staining, were therefore considered to represent cytosolic aggregates. Immunofluorescence showed that ectopic introduction of S888A (key PBD binding residue) single mutant or S861A-S888A double mutant of MLL5 failed to rescue PLK1 mislocalization, whereas wild-type MLL5 and S861A (phospho-site) mutant managed to reduce the proportion of cells with cytosolic PLK1 aggregates from 60.0% to 22.0% or 23.0%, respectively (Fig. 7, A and B; $P < 0.001$). Furthermore, reduction in fluorescence intensity of the centrosomal PLK1 in the MLL5-KD cells at prometaphase could be restored by overexpressing wild-type MLL5 or S861A mutant, but not S888A or S861A-S888A mutant (Fig. 7 C; $P < 0.001$). These results demonstrate that PBD binding to MLL5 on Ser-888 rather than PLK1 phosphorylating MLL5 on Ser-861 was essential for preventing aberrant cytosolic aggregation of PLK1.

Consistently, knockdown of MLL5 led to an increased proportion of cells displaying multiple centrosome markers with chro-

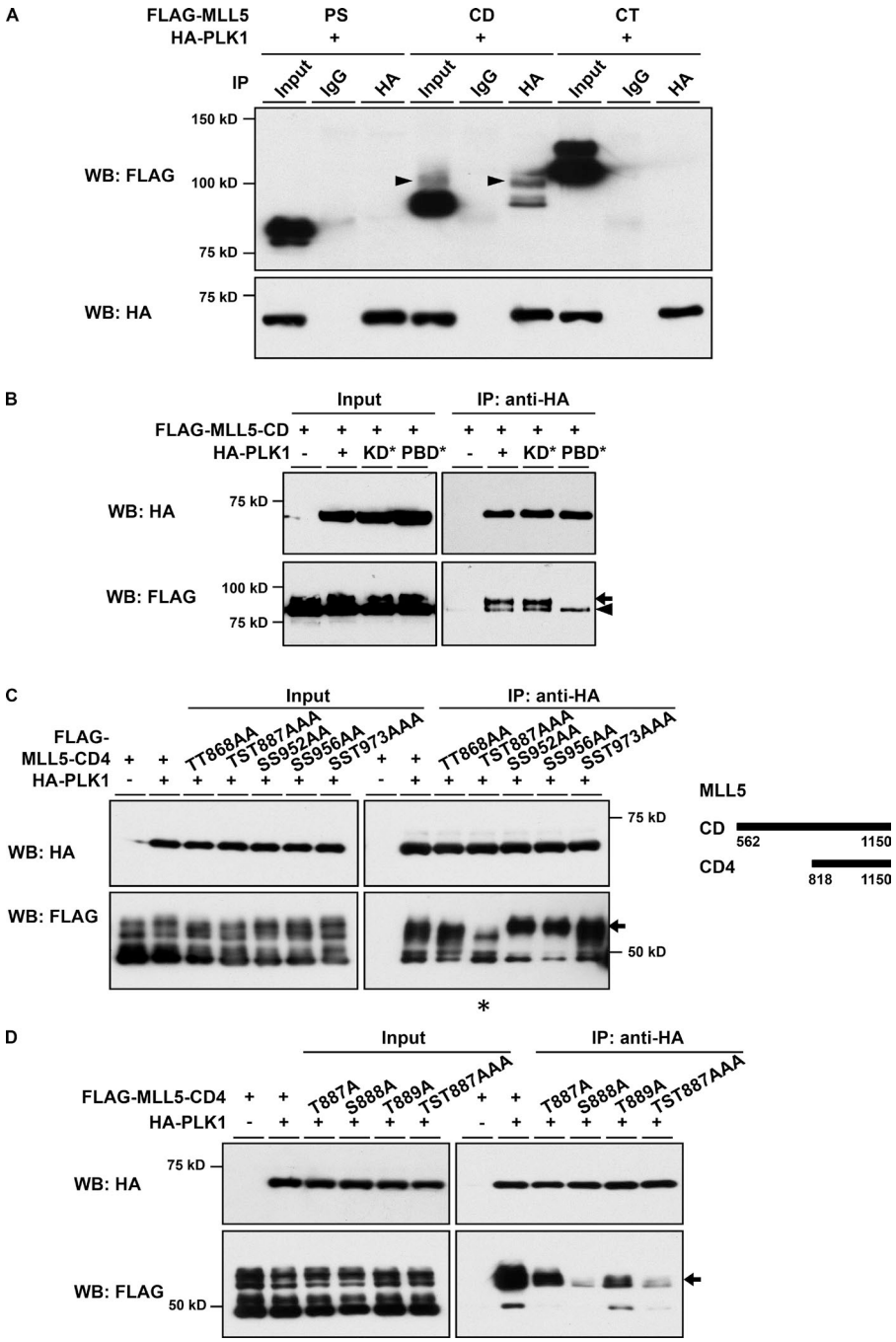

Figure 5. **The PLK1 PBD binds to the Thr887-Ser888-Thr889 motif on MLL5.** (A) The central domain of MLL5 binding to HA-PLK1. 293T cells expressing FLAG-MLL5 truncated mutant and HA-PLK1 were synchronized to prometaphase by nocodazole treatment. The cell lysates were immunoprecipitated with anti-HA antibody or mouse IgG and detected by Western blotting (WB) with anti-FLAG and anti-HA antibodies. Arrowhead indicates the slower-migrating form of FLAG-MLL5-CD. PS, PHD/SET domain; CT, C-terminal domain. (B) Loss of interaction between PBD-mutated PLK1 and the slowest-migrating form of FLAG-MLL5-CD. 293T cells expressing FLAG-MLL5-CD and HA-PLK1 or its mutants were synchronized to prometaphase. The cell lysates were immunoprecipitated with anti-HA antibody and detected by Western blotting with anti-FLAG and anti-HA antibodies. Arrowhead indicates the faster-migrating form of MLL5-CD; arrow indicates the slower-migrating form of MLL5-CD with PTMs. KD*, kinase dead; PBD*, PBD mutated. (C and D) Reduced interaction between PLK1 and the slowest-migrating form of TST887AAA, T887A, S888A, or T889A mutant. 293T cells expressing FLAG-MLL5-CD4 or its mutants and HA-PLK1 were synchronized to prometaphase before immunoprecipitation and Western blotting. Arrow indicates the slowest-migrating form of MLL5-CD4 or its mutant; * indicates the interaction between TST887AAA mutant and PLK1. Results are representative of at least three experimental repeats.

mosome misalignment (4.8% to 31.5%). Similar to the rescue of cytosolic PLK1 aggregation and centrosomal PLK1 signal reduction, exogenous expression of wild-type MLL5 or S861A mutant in MLL5-KD cells significantly decreased this proportion to 10.7% ($P = 0.005$) or 15.3% ($P = 0.012$), respectively. However, overexpression of either S888A single mutant or S861A-S888A double mutant failed to rescue multiple centrosome markers, with ∼30% of cells displaying multiple pericentrin foci ($P > 0.05$; Fig. 7, D and E). These data reveal that PLK1 PBD binding to MLL5 Ser-888, but not PLK1 phosphorylation of Ser-861, was required for the maintenance of spindle bipolarity. Collectively, the loss of PLK1 PBD binding to MLL5 led to the formation of cytosolic PLK1 aggregates, which in turn contributed to aMTOC formation.

Discussion

We reveal MLL5 to be a novel centrosome component that localizes to the centrosome throughout the cell cycle. PLK1 PBD binding to the Thr887-Ser888-Thr889 motif on MLL5 keeps PLK1 in a nonaggregated form at prometaphase and facilitates its incorporation to the centrosome during mitosis. In the absence of MLL5, the interaction between MLL5 and PLK1 is abolished, resulting in less soluble PLK1 in the cytosol. PLK1 therefore aggregates rather than being recruited to the centrosome. Some of these aggregates subsequently turn into aMTOCs, leading to spindle multipolarity at metaphase (Fig. 8).

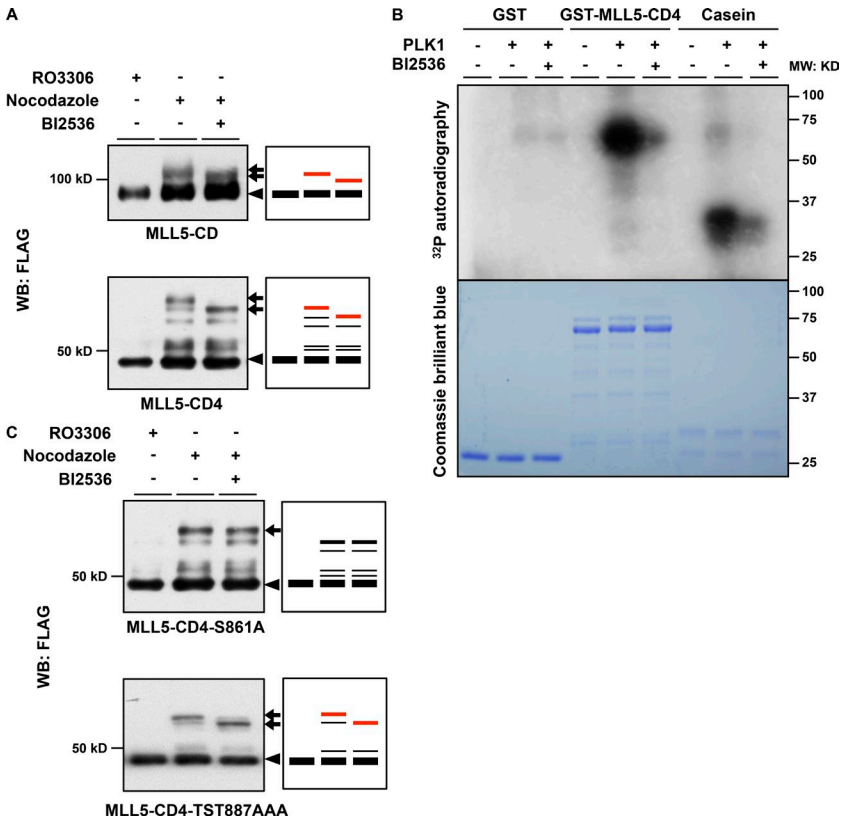

Figure 6. **PLK1 phosphorylates MLL5 on Ser-861.** (A) Gel mobility shift assay of MLL5-CD and MLL5-CD4. 293T cells expressing truncated FLAG-MLL5 mutant were treated with RO3306 or nocodazole in the presence or the absence of BI2536. The cell lysates were detected by Western blotting (WB) with anti-FLAG antibody. (B) PLK1 phosphorylation of MLL5 in vitro. (top) ^{32}P autoradiograph of in vitro PLK1 kinase assay. GST-MLL5-CD-4 purified from *E. coli* was subjected to an in vitro PLK1 kinase assay. BI2536 was introduced as an acute inhibitor of PLK1. GST and casein served as negative and positive controls, respectively. (bottom) Coomassie brilliant blue staining for GST, GST-MLL5-CD4, and Casein. (C) Gel mobility shift assay of MLL5-CD4-S861A and MLL5-CD4-TST887AAA. 293T cells expressing FLAG-MLL5-CD4 mutant were treated with RO3306 or nocodazole in the presence or absence of BI2536. Cell lysates were detected by WB with anti-FLAG antibody. Arrows in A and C indicate the slowest-migrating form of FLAG-MLL5 mutant. Arrowheads in A and C indicate the fastest-migrating form. Diagram in A and C illustrates the respective MLL5 migration patterns for the blot on the left. Results are representative of at least three experimental repeats.

Mitotic spindle multipolarity without centrosome amplification is mainly caused by centriole disengagement or PCM fragmentation (Maiato and Logarinho, 2014). However, the multipolar spindle formation observed in MLL5-KD cells does not fall into either of these categories. Immunofluorescence and time-lapse microscopy clearly showed the formation of aMTOCs, which subsequently became extra spindle poles. PLK1 is pivotal in centrosome-based microtubule nucleation. It recruits γ-tubulin to the centrosome and phosphorylates Nedd1 and Hice1 to promote Augmin–microtubule interaction (McInnes et al., 2006; Zhang et al., 2009a; Johmura et al., 2011). Because PLK1 formed cytosolic aggregates at prometaphase in MLL5-KD cells, it is likely that these mislocalized PLK1 served as additional microtubule nucleation sites, recruiting γ-TuRC and other PCM components during microtubule nucleation. These aMTOCs further organized microtubules to give rise to multipolar spindles at metaphase. Indeed, when MLL5-KD cells proceeded to metaphase, PLK1 localized to all the spindle poles, including those aMTOCs (Fig. 3 D). Moreover, MLL5 mutants incapable of binding to the PBD failed to rescue either cytosolic PLK1 aggregates or aMTOCs in MLL5-KD cells, further supporting that aMTOCs may be derived from cytosolic PLK1 aggregates in the absence of MLL5. Likewise, knockdown of centrosomal protein Numb also results in cytosolic PLK1 aggregation, which associates with γ-tubulin (Schmit et al., 2012). In MLL5-KD cells, PCM proteins were not recruited to PLK1 aggregates until metaphase (Fig. 3, A and D). This is probably because the prometaphase synchronization by nocodazole or monastrol treatment blocked the movement of PCM proteins along microtubules. Additionally, not all cytosolic PLK1 aggregates in MLL5-KD cells were able to recruit PCM proteins even at metaphase, likely because of insufficient kinase activity or binding ability of the PBD. More work needs to be done to elucidate the mechanism by which PLK1 aggregates lead to aMTOC formation in MLL5-KD cells.

The kinase activity of PLK1 is required for its recruitment to the centrosome (Lénart et al., 2007; Haren et al., 2009). Indeed, after we treated metaphase U2OS cells with BI2536, mitotic cells became monopolar and PLK1 dissociated from the centrosome, forming cytosolic aggregates (Fig. S4 B). Considering that PLK1 has several substrates and binding partners, we speculate that loss of interaction between PLK1 and its interacting proteins could possibly make cytosolic PLK1 less soluble and prone to aggregation. Thus, a smaller amount of PLK1 can be recruited to the kinetochore or the centrosome. Depletion of kinetochore-localized SENP6 resulted in PLK1 aggregates with reduced intensity of PLK1 at the kinetochore (Mukhopadhyay and Dasso, 2010). In contrast, knockdown of Numb causes PLK1 aggregation and impairs PLK1 spindle pole localization at both metaphase and anaphase (Schmit et al., 2012). In this study, knockdown of MLL5 disrupted the cytosolic interaction between MLL5 and PLK1, resulting in aberrant aggregation of PLK1 and partial dissociation from the centrosome. However, we also noted that endogenous MLL5 in BI2536-treated mitotic cells associated with PLK1 aggregates, suggesting a strong interaction between MLL5 and PLK1 that is independent of kinase activity (Fig. S4, C and D).

PLK1 PBD binding to phosphopeptides is believed to target PLK1 to specific subcellular localizations, including the centrosome (Elia et al., 2003a). However, Hanisch et al. (2006) showed that the PBD of PLK1 is dispensable during centrosome maturation. Another study found that the recruitment of PLK1 to the centrosome at the late G_2 phase, which initiates centrosome maturation, is dependent on PLK1 phosphorylation of pericentrin (Lee and Rhee, 2011). Yet this did not exclude the presence of alternative mechanisms for recruitment of PLK1 to the

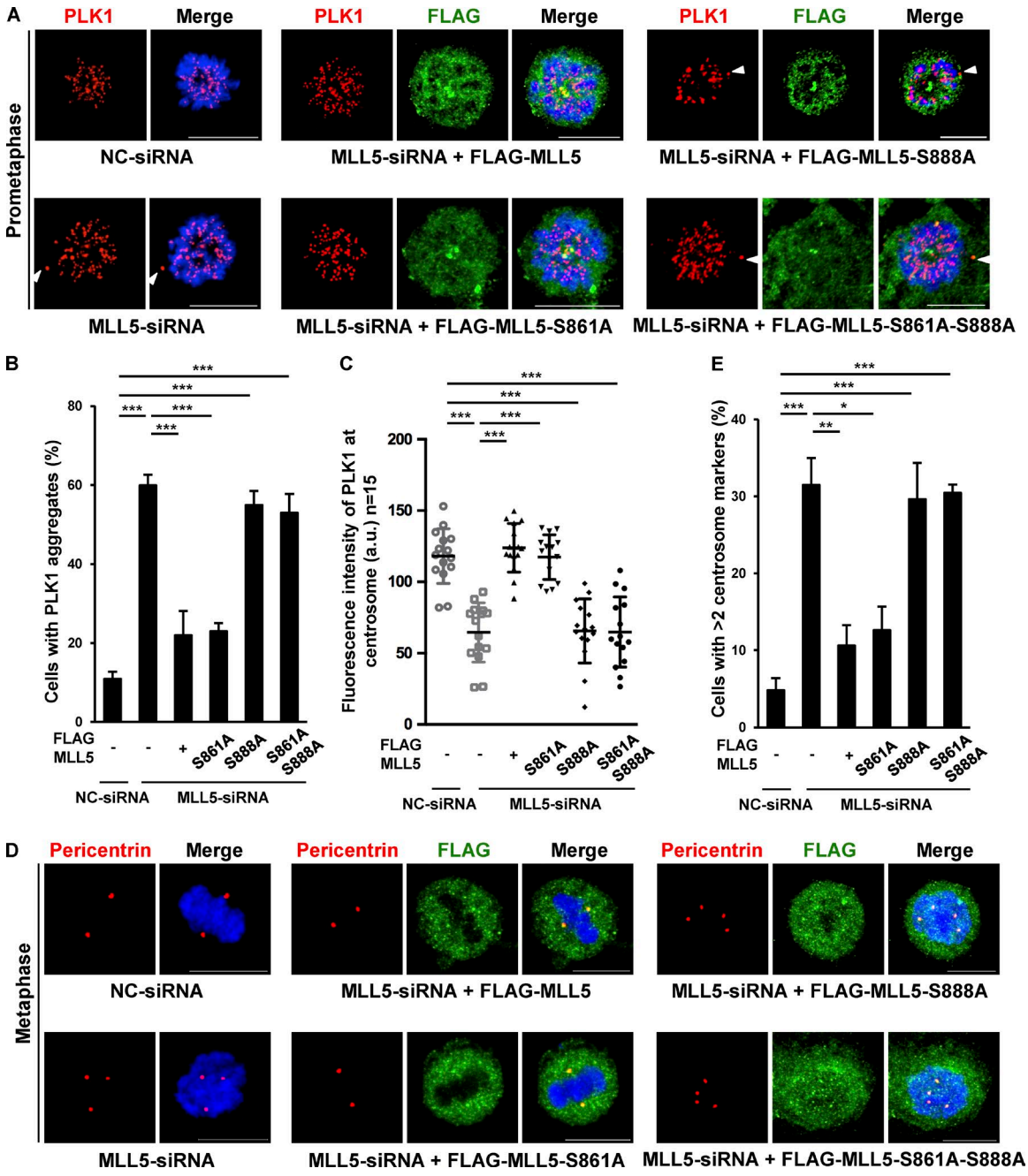

Figure 7. **Exogenous overexpression of MLL5 rescues PLK1 mislocalization and aMTOC formation in MLL5-KD cells.** (A) Overexpression of FLAG-MLL5 but not FLAG-MLL5 with S888A mutation rescuing PLK1 mislocalization in MLL5-KD cells. 293T cells were transfected with NC- or MLL5-siRNA for 16 h followed by overexpression of FLAG-MLL5 or its mutant for 8 h. The cells were then synchronized to prometaphase by monastrol treatment and immunostained for FLAG (green) and PLK1 (red). (B) Quantitation of the data presented in A. The experiments were repeated three times (n = 100 cells per sample). Error bars represent SEM. ***, $P < 0.001$. (C) Quantitation of centrosomal PLK1 signal at prometaphase in A. (a.u., arbitrary unit). 15 cells were captured per sample manually, and mean pixel intensity of PLK1 was computed. ***, $P < 0.001$. (D) Overexpression of FLAG-MLL5 but not FLAG-MLL5 with S888A mutation rescuing the formation of aMTOC in MLL5-KD cells. 293T cells were transfected with NC- or MLL5-siRNA for 16 h followed by overexpression of FLAG-MLL5 or its mutant for 8 h. After synchronization to metaphase by nocodazole-MG132 treatment, the cells were immunostained for FLAG (green) and pericentrin (red). (E) Quantitation of the data presented in D. The experiments were repeated three times (n = 100 cells per sample). Error bars represent SEM. *, $P < 0.05$; **, $P < 0.01$; ***, $P < 0.001$. DNA in A and D was counterstained with DAPI. Bars, 10 µm.

centrosome. In this study, rescue experiments showed that PLK1 binding to the Thr887-Ser888-Thr889 motif on MLL5, but not PLK1 phosphorylating MLL5 on Ser-861, had a dominant effect on PLK1 centrosomal localization. Although such binding occurs in the cytosol during mitosis, the centrosome-localized MLL5 may also interact with PLK1 and contribute to the incorporation of PLK1 into the centrosome. Moreover, we cannot exclude the possibility that phosphorylation of Ser-861 by PLK1 has other functions during mitosis. In addition, we observed a fast-migrating form of FLAG-MLL5-CD (Fig. 5 B), which maintained its ability to interact with PBD-mutated PLK1. This indicates that other PLK1 binding sites may exist on MLL5.

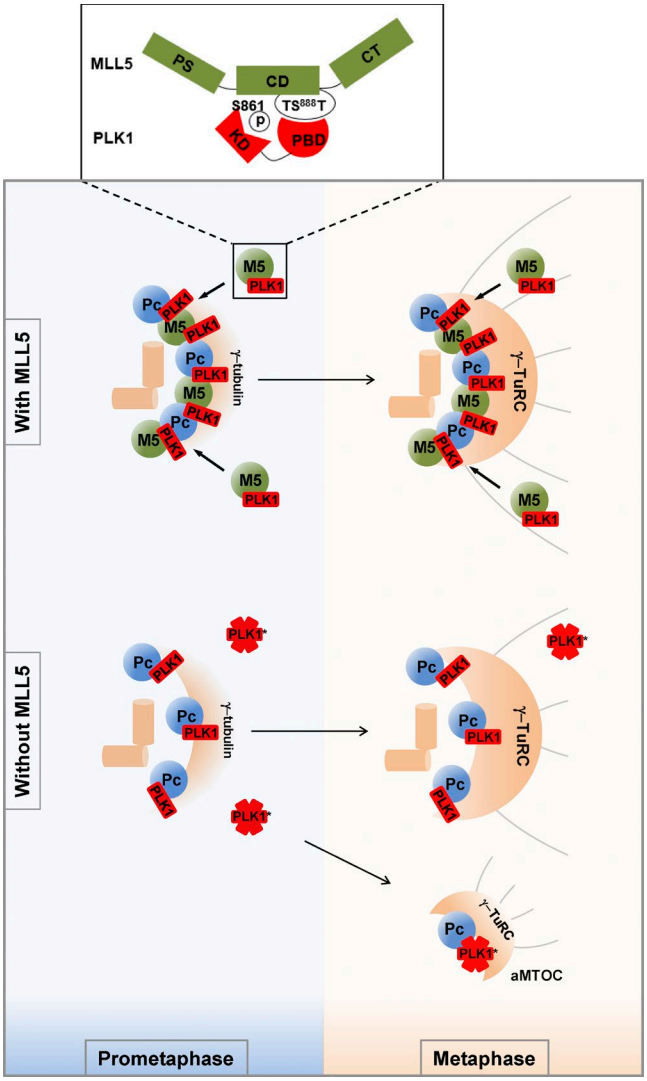

Figure 8. **Proposed working model for MLL5 maintaining spindle bipolarity.** Pc, pericentrin; M5, MLL5; γ-TuRC, γ-tubulin ring complex; PLK1*, PLK1 aggregates; PS, PHD/SET domain; CT, C-terminal domain; p, phosphorylated; KD, kinase domain; and TS888T, Thr887-Ser888-Thr889 motif on MLL5.

PLK1 is initially activated by Aurora A kinase phosphorylation in its T-loop with Bora, introducing a conformational change and disrupting autoinhibition of the kinase domain by the PBD (Jang et al., 2002; Macůrek et al., 2008; Seki et al., 2008). Binding of the PBD to phosphoproteins then induces PLK1 activity by further relieving the kinase domain from inhibition (Elia et al., 2003b). Indeed, the PLK1 PBD bound to the slower-migrating form of MLL5-CD (Fig. 5 A). Moreover, the Thr887-Ser888-Thr889-Pro890 motif falls into the consensus PBD-binding sequence: T/Q/H/M-S-pT/pS-P/X, where X stands for any amino acid (Elia et al., 2003a). However, phospho-mimicking mutant of MLL5 did not interact with the PBD (Fig. S3 D). One plausible explanation is that other modifications besides phosphorylation likely contribute to MLL5 interacting with the PBD. *O*-GlcNAcylation, acetylation, and *O*-sulfonation of serine/threonine have been discovered to transmit cell signal (Medzihradszky et al., 2004; Mittal et al., 2006; Mukherjee et al., 2006; Deplus et al., 2013). Recently, *O*-GlcNAcylation on two short forms of MLL5 has been identified (Ding et al., 2015; Nin et al., 2015). However, we could not rule out the possibility that phosphorylation on TST887 motif by a priming kinase is still required for MLL5 binding to the PBD of PLK1, because mutations to phospho-mimicking residue likely affected the overall structure of the motif. Although CDK1 phosphorylation of MLL5 on Thr-912 does not serve as a docking site for PBD binding, inhibition of CDK1 by RO3306 treatment abrogated the PBD binding to MLL5-CD4 (Fig. S4 E). CDK1 may activate a downstream target responsible for PLK1 PBD binding to MLL5. Discovery of PTMs required for PBD binding to MLL5 and identification of the enzyme involved would greatly advance our knowledge of PBD-mediated PLK1 function.

We observed that MLL5 localized to the centrosome throughout the cell cycle. Multiple slower-migrating forms of MLL5-CD4 were present at prometaphase (Fig. 5 D), and mass spectrometry identified 22 phosphorylated sites within the central domain of MLL5 (data not shown). Therefore, it is possible that MLL5 also serves as a substrate for other centrosomal kinases, facilitating their recruitment to the centrosome. Among the PLK family, PLK2 and PLK4 have been clearly demonstrated to regulate centriole duplication (Warnke et al., 2004; Bettencourt-Dias et al., 2005). Other kinases including Aurora A and Nek2 have also been shown to affect normal centrosome function or spindle bipolarity (Giet and Prigent, 2000; Garrett et al., 2002; Kufer et al., 2002; Eyers et al., 2003; Marumoto et al., 2003; Prigent et al., 2005; Asteriti et al., 2011; Cappello et al., 2014). Whether MLL5 plays a similar role in recruiting these kinases to the centrosome remains to be seen. Further exploration of the role of MLL5 in regulating the centrosome will strengthen our understanding of the critical mechanisms by which faithful bipolar spindle formation and genomic stability are achieved.

Materials and methods

Cell culture and synchronization

Osteosarcoma U2OS and embryonic kidney HEK 293T cells were cultured in DMEM supplemented with 10% FBS and 2 mM L-glutamine at 37°C in a humidified atmosphere of 5% CO_2. U2OS and 293T cells were synchronized to G_2 phase by incubation with 10 µM RO-3306 (217699; Calbiochem) and to prometaphase with 100 ng/ml nocodazole (M1404; Sigma-Aldrich) or 10 µM monastrol (M8515; Sigma-Aldrich) for 16 h. To collect mitotic U2OS cells, cells arrested at prometaphase were harvested using the mechanical shake-off procedure. Metaphase arrest was achieved by incubation with 100 ng/ml nocodazole for 16 h, followed by incubation in nocodazole-free medium with 20 µM MG132 for 90 min (474790; Calbiochem). To inhibit PLK1, 100 nM BI2536 (S1109; Selleck Chemicals) was applied to cells treated with nocodazole or MG132 for 90 min.

siRNA, DNA constructs, and transfection

siRNAs targeting MLL5 protein were designed as previously described (Cheng et al., 2008). MLL5 siRNA duplexes: sense, 5′-CGCCGGAAAAGGGAAAAUAdTdT-3′; antisense, 5′-UAUUUUCCCUUUUCCGGCGdTdT-3′ (targeting nucleotide position at 1,063 from the transcription starting point); sense, 5′-CAGCCCUCUGCAAACUUUCAGAAUUdTdT-3′; antisense, 5′-AAUUCUGAAAGUUUGCAGAGGGCUGdTdT-3′ (targeting nucleotide position at 5,215 from the transcription starting point). PLK4 siRNA duplexes: sense, 5′-AACUAUCUUGGAGCUUUAUAAdTdT-3′; antisense, 5′-UUAUAAAGCUCCAAGAUAGUUdTdT-3′ (targeting nucleotide position at 212 from the transcription starting point); sense, 5′-ACUCCUUUCAGACAUAUA

AGdTdT-3′; antisense, 5′-CUUAUAUGUCUGAAAGGAGUdTdT-3′ (targeting nucleotide position at 2,913 from the transcription starting point; Habedanck et al., 2005). Duplexes were synthesized by 1st BASE (Singapore) and used in combination. Scrambled siRNA (sense, 5′-UUCUCCGAACGUGUCACGUdTdT-3′; antisense, 5′-ACGUCA CACGUUCGGAGAAdTdT-3′) was used as a negative control. MLL5 and its deletion mutants were generated by flanking each PCR fragment of MLL5 cDNA with an N-terminal FLAG-tag and were cloned into the pEF6 vector (K9610-20; Invitrogen) using BamHI and XbaI sites. The CD4 domain was cloned into pGEX-4T3 vector (27-4583-01; GE Healthcare) using BamHI and NotI sites for the GST fusion recombinant protein expression. α-Tubulin cDNA sequence was cloned into the pEGFP-C1 vector (6085-1; Clontech) using HindIII and BamHI for GFP fusion protein expression. Full-length PLK1 cDNA was cloned into the pXJ40-HA mammalian expression vector (Manser et al., 1997) using NotI and KpnI sites. PLK1 point mutants, kinase-dead (D194A) and PBD-mutated (H538A-K540M), were constructed using the QuikChange site-directed mutagenesis kit (Stratagene). Plasmid transfections were performed using the calcium phosphate method in 293T cells, and GST fusion protein was expressed in the *E. coli* BL21 strain. Depletion of endogenous MLL5 was achieved by transfection of siRNA duplexes using Lipofectamine RNAiMAX (13667-150; Invitrogen) according to the manufacturer's instructions.

shRNA lentivirus production and transduction

MLL5-specific shRNA (sense, 5′-CCGGATGCTGAGAGAACAGTT TGAACTCGAGTTCAAACTGTTCTCTCAGCATTTTTTG-3′; antisense, 5′-AATTCAAAAAATGCTGAGAGAACAGTTTGAACTCGA GTTCAAACTGTTCTCTCAGCAT-3′), targeting nucleotide position at 1,556 from the transcription starting point), and Scrambled shRNA (sense; 5′-CCGGTTCTCCGAACGTGTCACGTGACTCGAGTCACG TCACACGTTCGGAGAATTTTTG-3′; antisense, 5′-AATTCAAAA ATTCTCCGAACGTGTCACGTGACTCGAGTCACGTCACACGTT CGGAGAA-3′) were synthesized by 1st BASE (Singapore). They were annealed and cloned into the pLKO.1 vector. For recombinant lentivirus production, 293FT cells were cotransfected with 6-µg targeting construct pLKO.1-NCshRNA or pLKO.1-MLL5shRNA, 5-µg packaging construct pCMV-dR8.91, and 2.5-µg envelope plasmid PMD.G by the calcium phosphate transfection method for 48 h. The lentivirus-containing medium was harvested and filtered through a 0.45-µm filter (WAKI 2053-025). For cell transduction, the virus-containing cell supernatant was diluted 1:1 in DMEM complete medium and added to U2OS cells. After 24-h incubation, cells were synchronized to mitosis for further experiments. All the lentiviral vectors were gifts from Academia Sinica.

RNA extraction, cDNA synthesis, and real-time PCR

The U2OS cell pellet was homogenized in TRIzol reagent (155967-026; Invitrogen). DNase I–treated RNA was converted to cDNA using the iScriptTM cDNA synthesis kit (170-8890; Bio-Rad Laboratories). The quantitative RT-PCR reaction was performed in an iQ5 Multicolor Real-Time PCR machine (Bio-Rad Laboratories) using iTaq universal SYBR green supermix (172-5120; Bio-Rad Laboratories) according to the manufacturer's instructions. Primers used were, for PLK4: forward, 5′-GGTGGTAGAGGTTTTCCTCTTGC-3′; reverse, 5′-CAG CACCAGGAGAATTCTCCATC-3′; for MLL5: forward, 5′-CCACCA CAAAAGAAAAAGGTTTCTC-3′; reverse, 5′-GTGTTGGTAAAG GTAGGCTAGC-3′; and for GAPDH: forward, 5′-GTGAAGGTCGGA GTCAACG-3′; reverse, 5′-TGAGGTCAATGAAGGGGTC-3′.

Antibodies

Anti-MLL5 rabbit polyclonal antibody was generated in-house against a peptide corresponding to aa 1,157–1,170 (Cheng et al., 2008) and was used throughout this study for Western blotting, immunoprecipitation, and immunofluorescence. Commercial primary antibodies used for Western blotting, immunoprecipitation, and immunofluorescence were rabbit anti-pericentrin (ab4448; Abcam), rabbit anti–γ-tubulin (T5192; Sigma-Aldrich), mouse anti–γ-tubulin (T3559; Sigma-Aldrich), mouse anti–α-tubulin (T9026; Sigma-Aldrich), human autoantibody against centromere (CREST; HCT-0100; ImmunoVision), mouse anti-PLK1 (sc-17783; Santa Cruz Biotechnology), goat anti-MLL5 (sc-18214 and sc-68636; Santa Cruz Biotechnology), mouse anti–FLAG M2 (F1804; Sigma-Aldrich), rabbit anti-HA (sc-805, Santa Cruz Biotechnology), mouse anti-HA (H9658; Sigma-Aldrich), and rabbit anti–centrin-2 (sc-27793-R; Santa Cruz Biotechnology). Anti–mouse IgG-HRP, anti–rabbit IgG-HRP (Life Technologies), or Alexa Fluor 488, 568, and 594 (A11001, A11008, A11011, A11014, and A11031; Invitrogen) were used as secondary antibodies for immunoblotting or immunofluorescence.

Immunofluorescence microscopy

HEK 293T cells or U2OS cells grown on polylysine-coated coverslips were washed with PBS and fixed with methanol at −20°C for 10 min. After rehydration with PBS for 10 min and blocking for 1 h in 5% BSA in PBS at RT, coverslips were incubated with primary antibodies diluted in blocking buffer at 4°C overnight, followed by three washes with 0.05% Tween-20 in PBS. Cells were then incubated with secondary antibodies conjugated with Alexa Fluor 488, 568, or 594 for 1 h at RT. After three washes with 0.05% Tween-20 in PBS, DNA was counterstained with DAPI (D1306; Invitrogen). Coverslips were mounted with FluorSave reagent (345789; Merck). Images were obtained using a confocal fluorescence microscope FV 1000 or FV 1200 (Olympus) equipped with a 60× Plan Achromat oil immersion objective (NA 1.25) and the built-in laser scanning unit or a confocal fluorescence microscope (LSM 700 or LSM 710; ZEISS) equipped with a 63× Plan Apochromat oil immersion objective (NA 1.4) and built-in laser scanning unit, at RT. Images were acquired using FLUOVIEW viewer software (Ver. 4.2; Olympus) or ZEN 2011 (ZEISS) and analyzed by Imaris 7.2.3 (Bitplane), ZEN 2011, or Image-Pro Plus (Media Cybernetics). Confocal *Z*-stacks were rendered in 3D using Imaris 7.2.3 to generate 3D reconstructions. For fluorescence intensity measurements, the region of interest was defined by drawing a circle (diameter: 800 nm) including the centrosome. In each cell, both centrosomes were measured and the mean value was recorded.

Time-lapse microscopy

U2OS cells stably expressing GFP–α-tubulin were cultured on glass-bottom 35-mm culture dishes (World Precision Instruments) and assembled in a stage-top incubator with 5% CO_2. Sequences of images were acquired every 1 min for 30 min using an inverted fluorescence microscope (Olympus) equipped with a 100× Plan Achromat oil immersion objective (NA 1.25) and a cooled charged coupled device camera (QImaging). Images were analyzed using Image-Pro Plus.

Microtubule regrowth assay

After transfection of NC- or MLL5-siRNA for 24 h, U2OS cells were synchronized to metaphase by 100 ng/ml nocodazole for 16 h and subsequent 20 µM MG132 for 1.5 h. Mitotic cells were washed with ice-cold medium and incubated on ice for 30 min to depolymerize microtubule. Microtubule regrowth was induced by replacing the cold medium with 37°C medium containing 20 µM MG132 for 1.5 h.

Immunoblotting and immunoprecipitation

To prepare whole-cell lysates, confluent cells were harvested from wells of a six-well plate, washed once with ice-cold PBS, lysed in Laemmli sample buffer containing 200 mM DTT, and subjected to Western blotting. For immunoprecipitation, confluent cells harvested

from 6- or 10-cm Petri dishes were lysed in mild lysis buffer supplemented with protease and phosphatase inhibitors (150 mM NaCl, 20 mM Tris-HCl, pH 8.0, 1% Triton X-100, 2 mM PMSF, 2 µg/ml leupeptin, 2 µg/ml aprotinin, 1 µg/ml pepstatin A, 1 mM Na_3VO_4, 5 mM NaF, and 10 mM β-glycerophosphate) followed by centrifugation at 12,000 *g* for 15 min. The supernatant was considered low-speed lysate (LSL). LSLs were further centrifuged at 95,000 rpm for 30 min with a TLA-100.3 rotor (Beckman Coulter), and the supernatant was considered high-speed lysate (HSL). Both LSL and HSL were precleared with TrueBlot Anti-Mouse Ig IP Beads (00-8811-25; Rockland Immunochemicals) for 15 min on ice and then incubated with 2 µg anti-MLL5 antibody, anti–γ-tubulin antibody, anti-FLAG antibody, or anti-HA antibody at 4°C for 3 h and with TrueBlot Anti-Mouse Ig IP Beads for another 2 h. The beads were then washed with mild lysis buffer three times before elution with Laemmli sample buffer.

Isolation of the centrosome

1.5×10^8 exponentially growing U2OS cells were harvested and incubated in medium with 10 µg/ml nocodazole plus 5 µg/ml cytochalasin B (C2743; Sigma-Aldrich) for 90 min. Cells were washed with ice-cold PBS and 8% sucrose in 0.1× PBS and then lysed with hypotonic lysis buffer (1 mM Tris, pH 8.0, 0.5% NP-40, 8 mM 2-mercaptoethanol, and protease inhibitors described earlier) for 20 min on ice. Lysed cells were centrifuged at 1,800 *g* for 3 min, and supernatants containing centrosomes were applied onto 2 ml of 20% Ficoll cushion (F4375; Sigma-Aldrich) followed by centrifugation at 30,000 *g* for 45 min in an ultracentrifuge (Optima L-90K; Beckman Coulter) equipped with an SW-28 rotor. The centrosomes concentrated in the 6-ml liquid above the Ficoll cushion were further purified by centrifugation through a discontinuous (70%, 50%, and 40%) sucrose gradient at 140,000 *g* for 90 min. Fractions of 0.5 ml were collected and analyzed by Western blotting.

GST pull-down, in vitro kinase assay, and mass spectrometry

Expression of GST-MLL5-CD4 was induced with 0.1 mM IPTG in *E. coli* (BL21) at 30°C for 3 h. After purification with Glutathione S-Sepharose beads (17-0756-01; GE Healthcare), an in vitro kinase assay was performed in 20 µl of kinase buffer at 30°C for 30 min containing 50 mM Tris-HCl, pH 7.5, 10 mM $MgCl_2$, 0.1 mg/ml BSA, 250 µM DTT, 0.1 mM ATP, 0.1 mM EDTA, 1 mM Na_3VO_4, 10 mM β-glycerophosphate, 10 µCi [γ-^{32}P]ATP (NEG502A250UC; PerkinElmer), 10 µg active PLK1 (V2841; Promega), and 4 µg casein (V2841; Promega), GST, or GST-MLL5-CD4. The reaction mixture was resolved on a 10% SDS polyacrylamide gel and visualized by autoradiography. Protein bands were excised and analyzed by mass spectrometry using a 5600 TripleTOF analyzer (QqTOF; AB SCIEX) at the Protein and Proteomics Centre, Department of Biological Sciences, National University of Singapore. Phosphorylation identification was performed with ProteinPilot 4.2 (AB SCIEX).

Statistical analysis

All data shown represent the mean value of three independent experiments. Error bars represent the SEM. P-values were obtained by *t* test and represent a comparison of all cells analyzed in the indicated cell populations. All statistical analyses were performed using IBM SPSS Statistics 19.

Online supplemental material

Fig. S1 shows that MLL5 is a centrosomal protein and down-regulation of MLL5 causes multipolar spindle formation. Fig. S2 demonstrates that MLL5 and PLK1 colocalize to the centrosome; knockdown of MLL5 results in PLK1 centrosomal signal reduction at prometaphase; and knockdown of PLK4 depletes centrosome and centrosomal MLL5. Fig. S3 characterizes that MLL5-CD interacts with PLK1 in the cytosol, and the Thr887-Ser888-Thr889 motif on MLL5-CD4 interacts with the PLK1 PBD. Fig. S4 shows that PLK1 phosphorylates MLL5 on Ser-861; PLK1 forms aggregates in BI2536-treated cells with MLL5; and inhibition of CDK1 abrogates MLL5-CD4 interaction with the PLK1 PBD. Videos 1 and 2 show the reconstruction of 3D volume of normal bipolar spindles in control cells and multipolar spindles in MLL5-KD cells, respectively. Videos 3 and 4 show the formation of normal MTOC in control cells and the formation of aMTOC in MLL5-KD cells, respectively. Video 5 shows the reconstruction of 3D volume of PLK1 localization in control cells. Videos 6 and 7 characterize PLK1 cytosolic aggregation in MLL5-KD cells at metaphase. Online supplemental material is available at http://www.jcb.org/cgi/content/full/jcb.201501021/DC1.

Acknowledgments

We thank K. McLaughlin of Insight Editing London for critical review of the manuscript.

This work is supported by Academic Research Fund Tier 1 grants (R-183-000-286-112 and R-183-000-337-112). Both W. Zhao and J. Liu are recipients of research scholarships from Yong Loo Lin School of Medicine, National University of Singapore.

The authors declare no competing financial interests.

Author contributions: W. Zhao conceived and designed the study, performed most of the experiments, analyzed the data, and wrote the paper; J. Liu conceived and designed the study, imaged U2OS cells, conducted sucrose gradient centrifugation experiments, and constructed PLK1 plasmids. X. Zhang constructed lentiviral expression plasmids, conducted qRT-PCR, and wrote the paper. L.-W. Deng conceived and designed the study and wrote the paper.

Submitted: 6 January 2015
Accepted: 12 February 2016

References

Ali, M., H. Rincón-Arano, W. Zhao, S.B. Rothbart, Q. Tong, S.M. Parkhurst, B.D. Strahl, L.W. Deng, M. Groudine, and T.G. Kutateladze. 2013. Molecular basis for chromatin binding and regulation of MLL5. *Proc. Natl. Acad. Sci. USA.* 110:11296–11301. http://dx.doi.org/10.1073/pnas.1310156110

Archambault, V., and D.M. Glover. 2009. Polo-like kinases: Conservation and divergence in their functions and regulation. *Nat. Rev. Mol. Cell Biol.* 10:265–275. http://dx.doi.org/10.1038/nrm2653

Asteriti, I.A., M. Giubettini, P. Lavia, and G. Guarguaglini. 2011. Aurora-A inactivation causes mitotic spindle pole fragmentation by unbalancing microtubule-generated forces. *Mol. Cancer.* 10:131. http://dx.doi.org/10.1186/1476-4598-10-131

Barr, F.A., H.H. Silljé, and E.A. Nigg. 2004. Polo-like kinases and the orchestration of cell division. *Nat. Rev. Mol. Cell Biol.* 5:429–440. http://dx.doi.org/10.1038/nrm1401

Bettencourt-Dias, M., and D.M. Glover. 2007. Centrosome biogenesis and function: Centrosomics brings new understanding. *Nat. Rev. Mol. Cell Biol.* 8:451–463. http://dx.doi.org/10.1038/nrm2180

Bettencourt-Dias, M., A. Rodrigues-Martins, L. Carpenter, M. Riparbelli, L. Lehmann, M.K. Gatt, N. Carmo, F. Balloux, G. Callaini, and D.M. Glover. 2005. SAK/PLK4 is required for centriole duplication and flagella development. *Curr. Biol.* 15:2199–2207. http://dx.doi.org/10.1016/j.cub.2005.11.042

Cappello, P., H. Blaser, C. Gorrini, D.C. Lin, A.J. Elia, A. Wakeham, S. Haider, P.C. Boutros, J.M. Mason, N.A. Miller, et al. 2014. Role of Nek2 on

centrosome duplication and aneuploidy in breast cancer cells. *Oncogene.* 33:2375–2384. http://dx.doi.org/10.1038/onc.2013.183

Cheng, F., J. Liu, S.H. Zhou, X.N. Wang, J.F. Chew, and L.W. Deng. 2008. RNA interference against mixed lineage leukemia 5 resulted in cell cycle arrest. *Int. J. Biochem. Cell Biol.* 40:2472–2481. http://dx.doi.org/10.1016/j.biocel.2008.04.012

Cheng, F., J. Liu, C. Teh, S.W. Chong, V. Korzh, Y.J. Jiang, and L.W. Deng. 2011. Camptothecin-induced downregulation of MLL5 contributes to the activation of tumor suppressor p53. *Oncogene.* 30:3599–3611. http://dx.doi.org/10.1038/onc.2011.71

Conduit, P.T., Z. Feng, J.H. Richens, J. Baumbach, A. Wainman, S.D. Bakshi, J. Dobbelaere, S. Johnson, S.M. Lea, and J.W. Raff. 2014. The centrosome-specific phosphorylation of Cnn by Polo/Plk1 drives Cnn scaffold assembly and centrosome maturation. *Dev. Cell.* 28:659–669. http://dx.doi.org/10.1016/j.devcel.2014.02.013

Damm, F., T. Oberacker, F. Thol, E. Surdziel, K. Wagner, A. Chaturvedi, M. Morgan, K. Bomm, G. Göhring, M. Lübbert, et al. 2011. Prognostic importance of histone methyltransferase MLL5 expression in acute myeloid leukemia. *J. Clin. Oncol.* 29:682–689. http://dx.doi.org/10.1200/JCO.2010.31.1118

Deng, L.W., I. Chiu, and J.L. Strominger. 2004. MLL 5 protein forms intranuclear foci, and overexpression inhibits cell cycle progression. *Proc. Natl. Acad. Sci. USA.* 101:757–762. http://dx.doi.org/10.1073/pnas.2036345100

Deplus, R., B. Delatte, M.K. Schwinn, M. Defrance, J. Méndez, N. Murphy, M.A. Dawson, M. Volkmar, P. Putmans, E. Calonne, et al. 2013. TET2 and TET3 regulate GlcNAcylation and H3K4 methylation through OGT and SET1/COMPASS. *EMBO J.* 32:645–655. http://dx.doi.org/10.1038/emboj.2012.357

Ding, X., W. Jiang, P. Zhou, L. Liu, X. Wan, X. Yuan, X. Wang, M. Chen, J. Chen, J. Yang, et al. 2015. Mixed lineage leukemia 5 (MLL5) protein stability is cooperatively regulated by O-GlcNac transferase (OGT) and ubiquitin specific protease 7 (USP7). *PLoS One.* 10:e0145023. http://dx.doi.org/10.1371/journal.pone.0145023

Dumont, S., and T.J. Mitchison. 2009. Force and length in the mitotic spindle. *Curr. Biol.* 19:R749–R761. http://dx.doi.org/10.1016/j.cub.2009.07.028

Elia, A.E., L.C. Cantley, and M.B. Yaffe. 2003a. Proteomic screen finds pSer/pThr-binding domain localizing Plk1 to mitotic substrates. *Science.* 299:1228–1231. http://dx.doi.org/10.1126/science.1079079

Elia, A.E., P. Rellos, L.F. Haire, J.W. Chao, F.J. Ivins, K. Hoepker, D. Mohammad, L.C. Cantley, S.J. Smerdon, and M.B. Yaffe. 2003b. The molecular basis for phosphodependent substrate targeting and regulation of Plks by the Polo-box domain. *Cell.* 115:83–95. http://dx.doi.org/10.1016/S0092-8674(03)00725-6

Emerling, B.M., J. Bonifas, C.P. Kratz, S. Donovan, B.R. Taylor, E.D. Green, M.M. Le Beau, and K.M. Shannon. 2002. MLL5, a homolog of *Drosophila trithorax* located within a segment of chromosome band 7q22 implicated in myeloid leukemia. *Oncogene.* 21:4849–4854. http://dx.doi.org/10.1038/sj.onc.1205615

Eyers, P.A., E. Erikson, L.G. Chen, and J.L. Maller. 2003. A novel mechanism for activation of the protein kinase Aurora A. *Curr. Biol.* 13:691–697. http://dx.doi.org/10.1016/S0960-9822(03)00166-0

Fang, X., and P. Zhang. 2011. Aneuploidy and tumorigenesis. *Semin. Cell Dev. Biol.* 22:595–601. http://dx.doi.org/10.1016/j.semcdb.2011.03.002

Fry, A.M., T. Mayor, and E.A. Nigg. 2000. Regulating centrosomes by protein phosphorylation. *Curr. Top. Dev. Biol.* 49:291–312. http://dx.doi.org/10.1016/S0070-2153(99)49014-3

Fukasawa, K. 2007. Oncogenes and tumour suppressors take on centrosomes. *Nat. Rev. Cancer.* 7:911–924. http://dx.doi.org/10.1038/nrc2249

Gallo, M., F.J. Coutinho, R.J. Vanner, T. Gayden, S.C. Mack, A. Murison, M. Remke, R. Li, N. Takayama, K. Desai, et al. 2015. MLL5 orchestrates a cancer self-renewal state by repressing the histone variant H3.3 and Globally reorganizing chromatin. *Cancer Cell.* 28:715–729. http://dx.doi.org/10.1016/j.ccell.2015.10.005

Garrett, S., K. Auer, D.A. Compton, and T.M. Kapoor. 2002. hTPX2 is required for normal spindle morphology and centrosome integrity during vertebrate cell division. *Curr. Biol.* 12:2055–2059. http://dx.doi.org/10.1016/S0960-9822(02)01277-0

Giet, R., and C. Prigent. 2000. The *Xenopus laevis* aurora/Ip11p-related kinase pEg2 participates in the stability of the bipolar mitotic spindle. *Exp. Cell Res.* 258:145–151. http://dx.doi.org/10.1006/excr.2000.4903

Gopalakrishnan, J., V. Mennella, S. Blachon, B. Zhai, A.H. Smith, T.L. Megraw, D. Nicastro, S.P. Gygi, D.A. Agard, and T. Avidor-Reiss. 2011. Sas-4 provides a scaffold for cytoplasmic complexes and tethers them in a centrosome. *Nat. Commun.* 2:359. http://dx.doi.org/10.1038/ncomms1367

Habedanck, R., Y.D. Stierhof, C.J. Wilkinson, and E.A. Nigg. 2005. The Polo kinase Plk4 functions in centriole duplication. *Nat. Cell Biol.* 7:1140–1146. http://dx.doi.org/10.1038/ncb1320

Hanisch, A., A. Wehner, E.A. Nigg, and H.H.W. Silljé. 2006. Different Plk1 functions show distinct dependencies on Polo-Box domain-mediated targeting. *Mol. Biol. Cell.* 17:448–459. http://dx.doi.org/10.1091/mbc.E05-08-0801

Haren, L., T. Stearns, and J. Lüders. 2009. Plk1-dependent recruitment of gamma-tubulin complexes to mitotic centrosomes involves multiple PCM components. *PLoS One.* 4:e5976. http://dx.doi.org/10.1371/journal.pone.0005976

Heuser, M., D.B. Yap, M. Leung, T.R. de Algara, A. Tafech, S. McKinney, J. Dixon, R. Thresher, B. Colledge, M. Carlton, et al. 2009. Loss of MLL5 results in pleiotropic hematopoietic defects, reduced neutrophil immune function, and extreme sensitivity to DNA demethylation. *Blood.* 113:1432–1443. http://dx.doi.org/10.1182/blood-2008-06-162263

Ikeda, M., S. Chiba, K. Ohashi, and K. Mizuno. 2012. Furry protein promotes aurora A-mediated Polo-like kinase 1 activation. *J. Biol. Chem.* 287:27670–27681. http://dx.doi.org/10.1074/jbc.M112.378968

Jang, Y.J., C.Y. Lin, S. Ma, and R.L. Erikson. 2002. Functional studies on the role of the C-terminal domain of mammalian polo-like kinase. *Proc. Natl. Acad. Sci. USA.* 99:1984–1989. http://dx.doi.org/10.1073/pnas.042689299

Johmura, Y., N.K. Soung, J.E. Park, L.R. Yu, M. Zhou, J.K. Bang, B.Y. Kim, T.D. Veenstra, R.L. Erikson, and K.S. Lee. 2011. Regulation of microtubule-based microtubule nucleation by mammalian polo-like kinase 1. *Proc. Natl. Acad. Sci. USA.* 108:11446–11451. http://dx.doi.org/10.1073/pnas.1106223108

Kufer, T.A., H.H. Silljé, R. Körner, O.J. Gruss, P. Meraldi, and E.A. Nigg. 2002. Human TPX2 is required for targeting Aurora-A kinase to the spindle. *J. Cell Biol.* 158:617–623. http://dx.doi.org/10.1083/jcb.200204155

Lee, K., and K. Rhee. 2011. PLK1 phosphorylation of pericentrin initiates centrosome maturation at the onset of mitosis. *J. Cell Biol.* 195:1093–1101. http://dx.doi.org/10.1083/jcb.201106093

Lemak, A., A. Yee, H. Wu, D. Yap, H. Zeng, L. Dombrovski, S. Houliston, S. Aparicio, and C.H. Arrowsmith. 2013. Solution NMR structure and histone binding of the PHD domain of human MLL5. *PLoS One.* 8:e77020. http://dx.doi.org/10.1371/journal.pone.0077020

Lénárt, P., M. Petronczki, M. Steegmaier, B. Di Fiore, J.J. Lipp, M. Hoffmann, W.J. Rettig, N. Kraut, and J.M. Peters. 2007. The small-molecule inhibitor BI 2536 reveals novel insights into mitotic roles of polo-like kinase 1. *Curr. Biol.* 17:304–315. http://dx.doi.org/10.1016/j.cub.2006.12.046

Liu, J., X.N. Wang, F. Cheng, Y.C. Liou, and L.W. Deng. 2010. Phosphorylation of mixed lineage leukemia 5 by CDC2 affects its cellular distribution and is required for mitotic entry. *J. Biol. Chem.* 285:20904–20914. http://dx.doi.org/10.1074/jbc.M109.098558

Liu, J., F. Cheng, and L.W. Deng. 2012. MLL5 maintains genomic integrity by regulating the stability of the chromosomal passenger complex through a functional interaction with Borealin. *J. Cell Sci.* 125:4676–4685. http://dx.doi.org/10.1242/jcs.110411

Lowery, D.M., D. Lim, and M.B. Yaffe. 2005. Structure and function of Polo-like kinases. *Oncogene.* 24:248–259. http://dx.doi.org/10.1038/sj.onc.1208280

Lowery, D.M., K.R. Clauser, M. Hjerrild, D. Lim, J. Alexander, K. Kishi, S.E. Ong, S. Gammeltoft, S.A. Carr, and M.B. Yaffe. 2007. Proteomic screen defines the Polo-box domain interactome and identifies Rock2 as a Plk1 substrate. *EMBO J.* 26:2262–2273. http://dx.doi.org/10.1038/sj.emboj.7601683

Macůrek, L., A. Lindqvist, D. Lim, M.A. Lampson, R. Klompmaker, R. Freire, C. Clouin, S.S. Taylor, M.B. Yaffe, and R.H. Medema. 2008. Polo-like kinase-1 is activated by aurora A to promote checkpoint recovery. *Nature.* 455:119–123. http://dx.doi.org/10.1038/nature07185

Madan, V., B. Madan, U. Brykczynska, F. Zilbermann, K. Hogeveen, K. Döhner, H. Döhner, O. Weber, C. Blum, H.R. Rodewald, et al. 2009. Impaired function of primitive hematopoietic cells in mice lacking the mixed-lineage-leukemia homolog MLL5. *Blood.* 113:1444–1454. http://dx.doi.org/10.1182/blood-2008-02-142638

Maiato, H., and E. Logarinho. 2014. Mitotic spindle multipolarity without centrosome amplification. *Nat. Cell Biol.* 16:386–394. http://dx.doi.org/10.1038/ncb2958

Manser, E., H.Y. Huang, T.H. Loo, X.Q. Chen, J.M. Dong, and T. Leung. 1997. Expression of constitutively active αPAK reveals effects of the kinases and focal complexes. *Mol. Cell Biol.* 17:1129–1143. http://dx.doi.org/10.1128/MCB.17.3.1129

Marumoto, T., S. Honda, T. Hara, M. Nitta, T. Hirota, E. Kohmura, and H. Saya. 2003. Aurora-A kinase maintains the fidelity of early and late mitotic events in HeLa cells. *J. Biol. Chem.* 278:51786–51795. http://dx.doi.org/10.1074/jbc.M306275200

McInnes, C., A. Mazumdar, M. Mezna, C. Meades, C. Midgley, F. Scaerou, L. Carpenter, M. Mackenzie, P. Taylor, M. Walkinshaw, et al. 2006. Inhibitors of Polo-like kinase reveal roles in spindle-pole maintenance. *Nat. Chem. Biol.* 2:608–617. http://dx.doi.org/10.1038/nchembio825

Medzihradszky, K.F., Z. Darula, E. Perlson, M. Fainzilber, R.J. Chalkley, H. Ball, D. Greenbaum, M. Bogyo, D.R. Tyson, R.A. Bradshaw, and A.L. Burlingame. 2004. O-sulfonation of serine and threonine: Mass spectrometric detection and characterization of a new posttranslational modification in diverse proteins throughout the eukaryotes. *Mol. Cell. Proteomics.* 3:429–440. http://dx.doi.org/10.1074/mcp.M300140-MCP200

Mittal, R., S.Y. Peak-Chew, and H.T. McMahon. 2006. Acetylation of MEK2 and I kappa B kinase (IKK) activation loop residues by YopJ inhibits signaling. *Proc. Natl. Acad. Sci. USA.* 103:18574–18579. http://dx.doi.org/10.1073/pnas.0608995103

Mukherjee, S., G. Keitany, Y. Li, Y. Wang, H.L. Ball, E.J. Goldsmith, and K. Orth. 2006. Yersinia YopJ acetylates and inhibits kinase activation by blocking phosphorylation. *Science.* 312:1211–1214. http://dx.doi.org/10.1126/science.1126867

Mukhopadhyay, D., and M. Dasso. 2010. The fate of metaphase kinetochores is weighed in the balance of SUMOylation during S phase. *Cell Cycle.* 9:3194–3201. http://dx.doi.org/10.4161/cc.9.16.12619

Neef, R., U. Gruneberg, R. Kopajtich, X. Li, E.A. Nigg, H. Sillje, and F.A. Barr. 2007. Choice of Plk1 docking partners during mitosis and cytokinesis is controlled by the activation state of Cdk1. *Nat. Cell Biol.* 9:436–444. http://dx.doi.org/10.1038/ncb1557

Nin, D.S., W. Huang, M. Ali, C.W. Yew, T.G. Kutateladze, and L.W. Deng. 2015. O-GlcNAcylation of MLL5β is essential for MLL5β-AP-1 transcription complex assembly at the HPV16/18-long control region. *J. Mol. Cell Biol.* 7:180–183. http://dx.doi.org/10.1093/jmcb/mjv009

Oshimori, N., M. Ohsugi, and T. Yamamoto. 2006. The Plk1 target Kizuna stabilizes mitotic centrosomes to ensure spindle bipolarity. *Nat. Cell Biol.* 8:1095–1101. http://dx.doi.org/10.1038/ncb1474

Petronczki, M., P. Lénárt, and J.M. Peters. 2008. Polo on the rise-from mitotic entry to cytokinesis with Plk1. *Dev. Cell.* 14:646–659. http://dx.doi.org/10.1016/j.devcel.2008.04.014

Pihan, G.A. 2013. Centrosome dysfunction contributes to chromosome instability, chromoanagenesis, and genome reprograming in cancer. *Front. Oncol.* 3:277. http://dx.doi.org/10.3389/fonc.2013.00277

Preisinger, C., R. Körner, M. Wind, W.D. Lehmann, R. Kopajtich, and F.A. Barr. 2005. Plk1 docking to GRASP65 phosphorylated by Cdk1 suggests a mechanism for Golgi checkpoint signalling. *EMBO J.* 24:753–765. http://dx.doi.org/10.1038/sj.emboj.7600569

Prigent, C., D.M. Glover, and R. Giet. 2005. Drosophila Nek2 protein kinase knock-down leads to centrosome maturation defects while overexpression causes centrosome fragmentation and cytokinesis failure. *Exp. Cell Res.* 303:1–13.

Schmit, T.L., M. Nihal, M. Ndiaye, V. Setaluri, V.S. Spiegelman, and N. Ahmad. 2012. Numb regulates stability and localization of the mitotic kinase PLK1 and is required for transit through mitosis. *Cancer Res.* 72:3864–3872. http://dx.doi.org/10.1158/0008-5472.CAN-12-0714

Sebastian, S., P. Sreenivas, R. Sambasivan, S. Cheedipudi, P. Kandalla, G.K. Pavlath, and J. Dhawan. 2009. MLL5, a trithorax homolog, indirectly regulates H3K4 methylation, represses cyclin A2 expression, and promotes myogenic differentiation. *Proc. Natl. Acad. Sci. USA.* 106:4719–4724. http://dx.doi.org/10.1073/pnas.0807136106

Seki, A., J.A. Coppinger, C.Y. Jang, J.R. Yates, and G. Fang. 2008. Bora and the kinase Aurora A cooperatively activate the kinase Plk1 and control mitotic entry. *Science.* 320:1655–1658. http://dx.doi.org/10.1126/science.1157425

Sumara, I., J.F. Giménez-Abián, D. Gerlich, T. Hirota, C. Kraft, C. de la Torre, J. Ellenberg, and J.M. Peters. 2004. Roles of polo-like kinase 1 in the assembly of functional mitotic spindles. *Curr. Biol.* 14:1712–1722. http://dx.doi.org/10.1016/j.cub.2004.09.049

van Vugt, M.A., B.C. van de Weerdt, G. Vader, H. Janssen, J. Calafat, R. Klompmaker, R.M. Wolthuis, and R.H. Medema. 2004. Polo-like kinase-1 is required for bipolar spindle formation but is dispensable for anaphase promoting complex/Cdc20 activation and initiation of cytokinesis. *J. Biol. Chem.* 279:36841–36854. http://dx.doi.org/10.1074/jbc.M313681200

Vitre, B.D., and D.W. Cleveland. 2012. Centrosomes, chromosome instability (CIN) and aneuploidy. *Curr. Opin. Cell Biol.* 24:809–815. http://dx.doi.org/10.1016/j.ceb.2012.10.006

Warnke, S., S. Kemmler, R.S. Hames, H.L. Tsai, U. Hoffmann-Rohrer, A.M. Fry, and I. Hoffmann. 2004. Polo-like kinase-2 is required for centriole duplication in mammalian cells. *Curr. Biol.* 14:1200–1207. http://dx.doi.org/10.1016/j.cub.2004.06.059

Woodruff, J.B., O. Wueseke, V. Viscardi, J. Mahamid, S.D. Ochoa, J. Bunkenborg, P.O. Widlund, A. Pozniakovsky, E. Zanin, S. Bahmanyar, et al. 2015. Centrosomes. Regulated assembly of a supramolecular centrosome scaffold in vitro. *Science.* 348:808–812. http://dx.doi.org/10.1126/science.aaa3923

Wueseke, O., J. Bunkenborg, M.Y. Hein, A. Zinke, V. Viscardi, J.B. Woodruff, K. Oegema, M. Mann, J.S. Andersen, and A.A. Hyman. 2014. The *Caenorhabditis elegans* pericentriolar material components SPD-2 and SPD-5 are monomeric in the cytoplasm before incorporation into the PCM matrix. *Mol. Biol. Cell.* 25:2984–2992. http://dx.doi.org/10.1091/mbc.E13-09-0514

Yap, D.B., D.C. Walker, L.M. Prentice, S. McKinney, G. Turashvili, K. Mooslehner-Allen, T.R. de Algara, J. Fee, X. de Tassigny, W.H. Colledge, and S. Aparicio. 2011. Mll5 is required for normal spermatogenesis. *PLoS One.* 6:e27127. http://dx.doi.org/10.1371/journal.pone.0027127

Zhang, X., Q. Chen, J. Feng, J. Hou, F. Yang, J. Liu, Q. Jiang, and C. Zhang. 2009a. Sequential phosphorylation of Nedd1 by Cdk1 and Plk1 is required for targeting of the gammaTuRC to the centrosome. *J. Cell Sci.* 122:2240–2251. http://dx.doi.org/10.1242/jcs.042747

Zhang, Y., J. Wong, M. Klinger, M.T. Tran, K.M. Shannon, and N. Killeen. 2009b. MLL5 contributes to hematopoietic stem cell fitness and homeostasis. *Blood.* 113:1455–1463. http://dx.doi.org/10.1182/blood-2008-05-159905

Zhou, P., Z. Wang, X. Yuan, C. Zhou, L. Liu, X. Wan, F. Zhang, X. Ding, C. Wang, S. Xiong, et al. 2013. Mixed lineage leukemia 5 (MLL5) protein regulates cell cycle progression and E2F1-responsive gene expression via association with host cell factor-1 (HCF-1). *J. Biol. Chem.* 288:17532–17543. http://dx.doi.org/10.1074/jbc.M112.439729